Directivity models in the NGA-West2 Project

Paul Spudich
US Geological Survey, Menlo Park, CA

National Seismic Hazard Mapping Project

Dec. 13, 2012

This study was sponsored by the Pacific Earthquake Engineering Research Center (PEER) and funded by the California Earthquake Authority, California Department of Transportation, and the Pacific Gas & Electric Company. Any opinions, findings, and conclusions or recommendations expressed in this material are those of the authors and do not necessarily reflect those of the above mentioned agencies.

NGA-West2 Directivity Modelers

- all contributed results and slides

- Jack Baker and Shrey Shahi, Stanford
- Jeff Bayless and Paul Somerville, URS
- Badie Rowshandel, CGS and CEA
- Paul Spudich (USGS) and Brian Chiou (CalTrans)

(Not part of NGA West 2, working in parallel:)

- Jennie Watson-Lamprey (JWL Consulting)

  (still under development; will not discuss today)

	Model	Scales properly for large faults?	Comps of motion of PSA	Band width	Have avg model ?	Other features
Old	Somerville et al (1997)	No	FN, FP. Geomean	broad	no	Granddaddy of them all. But normalized to fault dimension.
	Abrahamson (2000)	No, but...	FN, FP. Geomean	broad	no	Normalized, but capped to partially solve scaling problem
	Spudich and Chiou (2008)	**Yes**	Gmroti50 (FN, FP*)	broad	no	* Can calculate FN and FP, but not checked against data
New	Bayless and Somerville (2013)	**Yes**	FN, FP, Rotd50	broad	no	Uses simple directivity predictors similar to Somerville etal 97. Use for complicated fault geometries is approximated. Fit to four NGA-1 GMPEs. Probably vulnerable to 'closest point' discontinuities.
	Rowshandel (2013)	**Yes**	Rotd50	broad	no	Provides spatially smoothest maps of directivity, can handle complicated geometries, but requires integral over fault surface.
	Shahi and Baker (2013)	Maybe	FN**, Rotd50	**narrow**	**Yes**	This is a pulse model, which is not identical to directivity. Probably vulnerable to 'closest point' discontinuities, but they may be less severe because 'directivity' amplification occurs only at small R. ** They have a separate polarization model.
	Spudich and Chiou (2013)	**Yes**	Rotd50, (FN, FP*)	**narrow**	no	Implementation rather complicated. Vulnerable to 'closest point' discontinuities. The most physically motivated of the models.

Status of the Directivity Models

Preliminary directivity models (functional forms, (DFFs), and approximate coefficients) have been developed by each of the NGA West 2 modeler teams based on sets of ground motion intra-event residuals, typically with respect to the NGA 2008 GMPEs

Final coefficients are to be determined by the GMPE developers (with big caveat)

All ‘amplitudes’ of directivity in this talk will change if/when the GMPE developers solve for the coefficients
– look at the spatial patterns, not the amplitudes!

Which directivity models will be in which GMPE?

Use of models that calculate directivity for a specific hypocenter:
B. Chiou and R. Youngs will determine coefficients for a directivity functional form (DFF) which will be either the

- Spudich and Chiou IDP-based directivity model or the
- Spudich and Chiou IEP model (in development).

Directivity models that average over a distribution of hypocenters:
Some GMPE developers are reluctant to add a directivity model that requires a hypocenter location, because that adds another loop over hypocenter position to their PSHA codes. Shahi and Baker have an interesting average model.

Jennie Watson-Lamprey has been investigating whether directivity of an ensemble of ruptures having different hypocenters can be modeled by a position-dependent sigma**. Preliminary results look promising**.

She has also been comparing the reduction in aleatory sigma caused by the different directivity models, which has been very encouraging (to me).

Comparison of predicted directivity amplification on various hypothetical test earthquakes

Conclusions:

The considered models are fairly similar for vertical strike-slip faults.

Directivity model predictions start diverging for dipping faults.

The maps of directivity show that for dipping faults the model predictions are more strongly controlled by model assumptions than by data.

It would be unwise to use just one model for site-specific predictions near a fault dipping < 60? degrees.

M7.9 Denali Earthquake, Spudich & Chiou IDP model 3

Amplification factor for 5 s SA shown

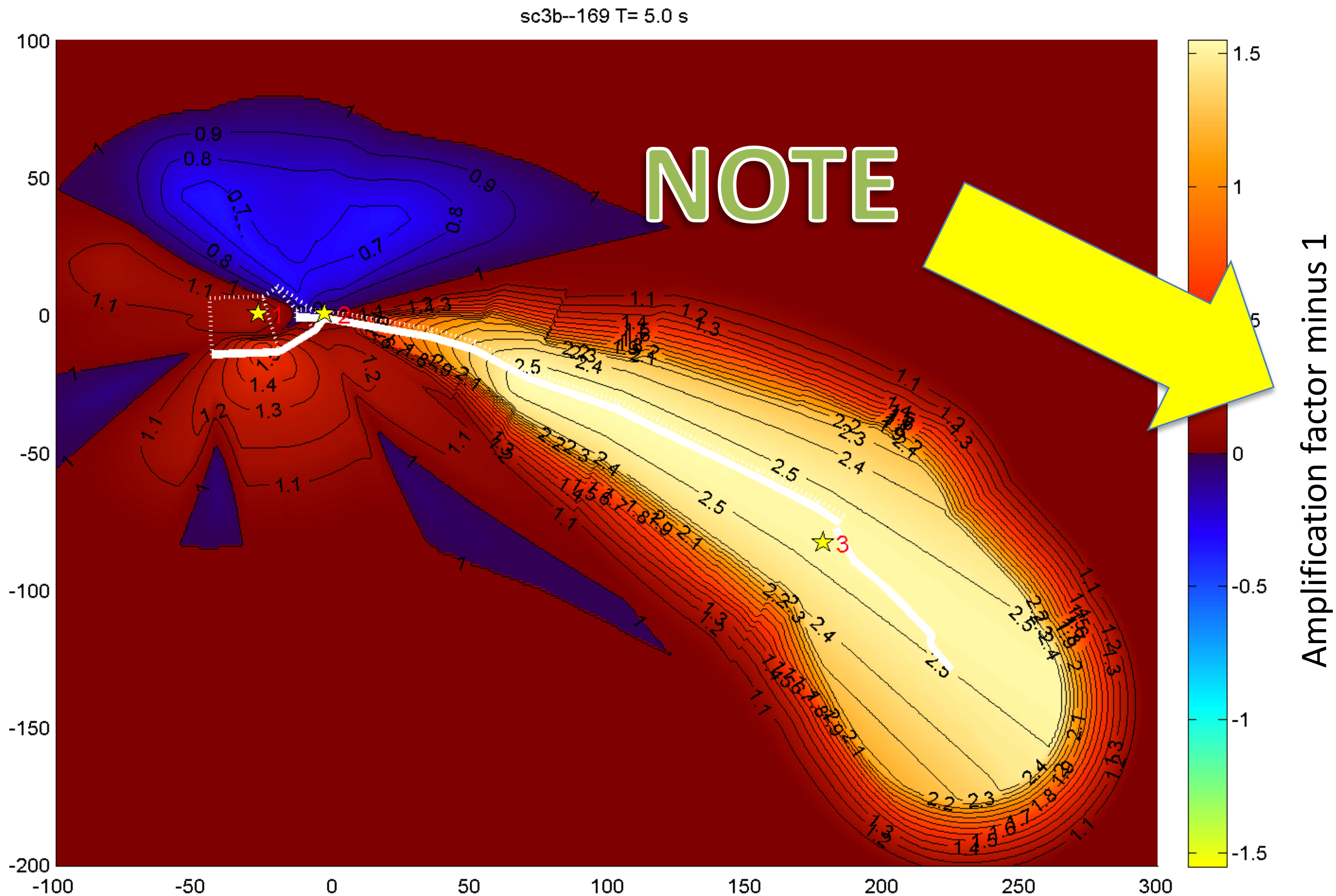

Amplification factors shown here are not necessarily factors applied to an existing GMPE!!

Existing GMPEs already have some directivity in them!!

This gets into the ‘centering’ problem.

Ground motion amplification factor for rupture geometry ss3, M 7.2, comparing models sha12, sc3b, and row12. This picture is fairly typical of all strike-slip test geometries

ALL R RESULTS HAVE CONSTANT OFFSET

Shahi and Baker

Spudich and Chiou (model 3)

Rowshandel

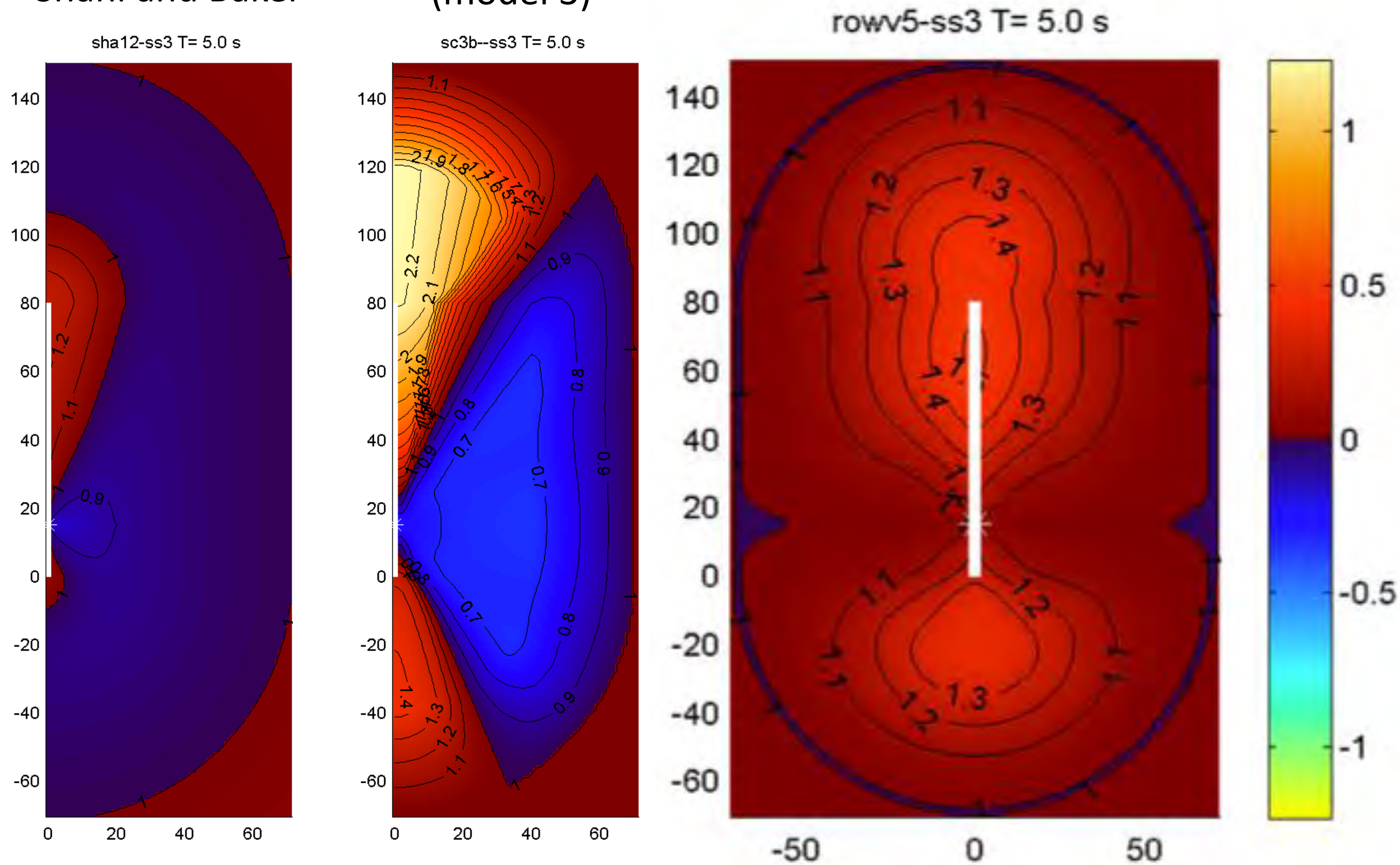

Comparison of predicted directivity from models sha12, sc3b, and row12 for M7.2 steeply-dipping oblique-slip test model so6 (rake = 135°).

Shahi and Baker

Spudich and Chiou (model 3)

Rowshandel

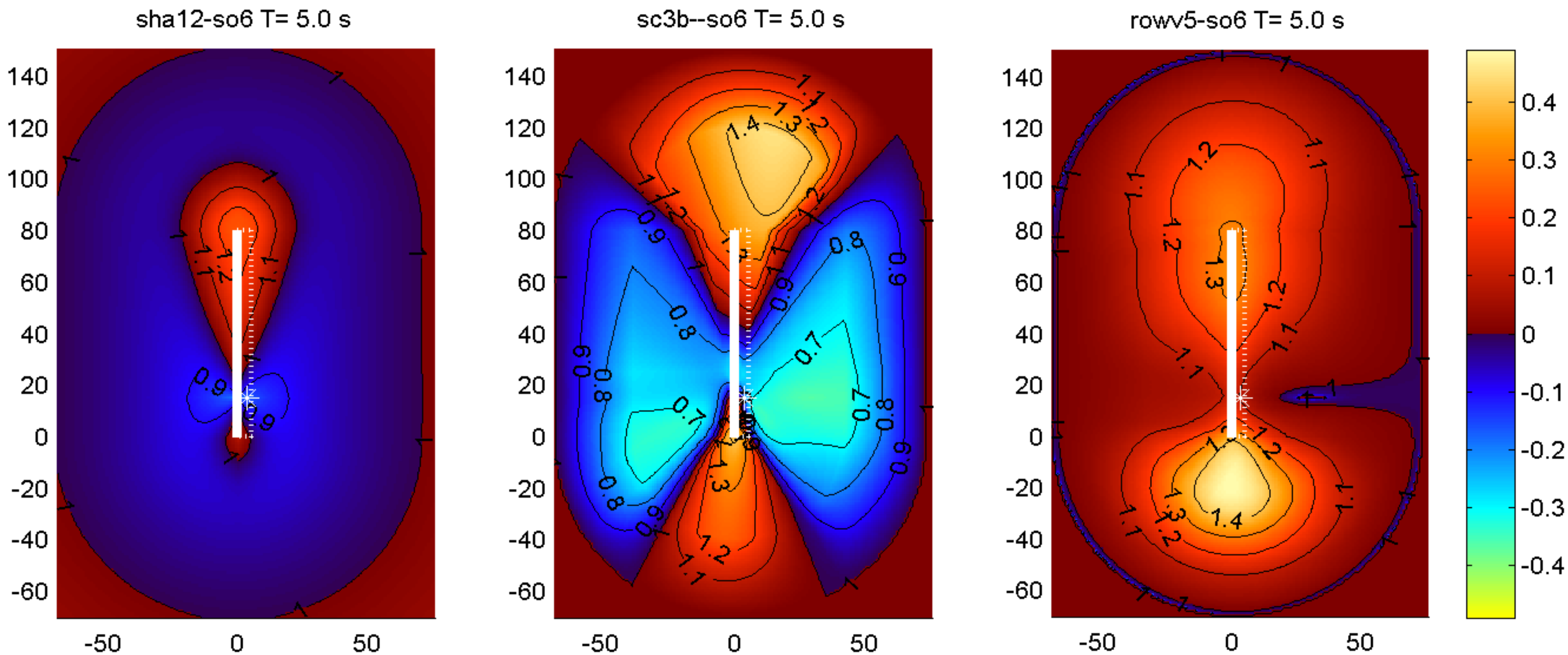

Normalized fault dimension in Somerville et al. (1997)

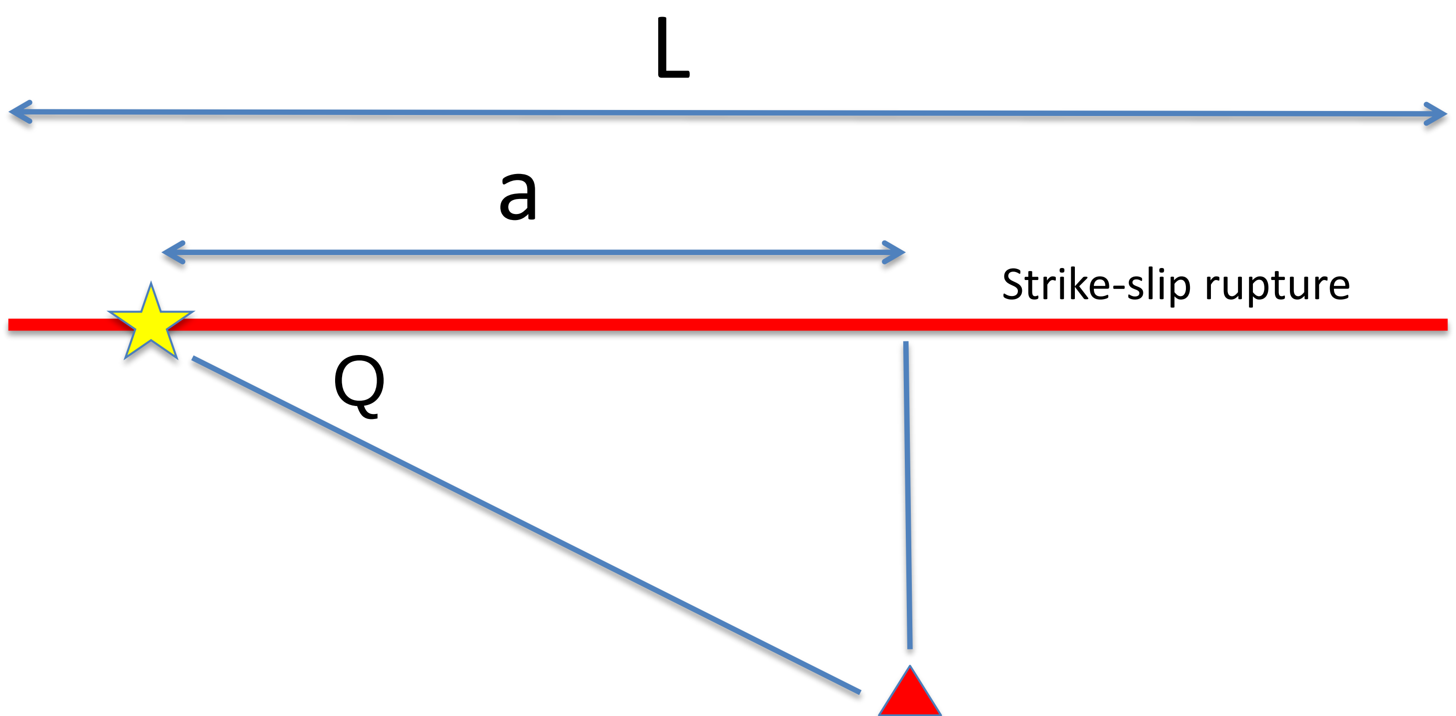

$$X = {}^{a}\!/_{L}\,,\ \text{directivity parameter} = X\cos Q$$

Scaling flaw in some earlier models:

- Normalized Fault Dimensions Problematic

Directivity models based on normalized fault do not scale properly when applied to very long strike-slip earthquakes.

For example

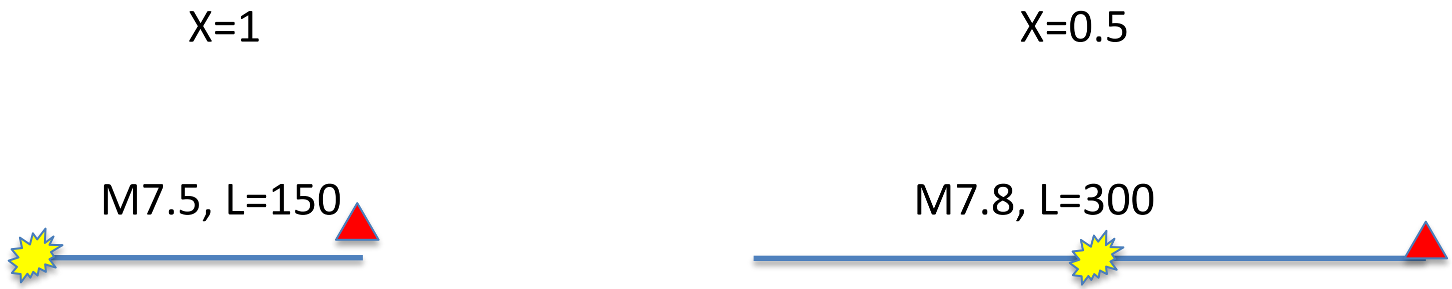

All NGA West 2 directivity models have fixed the problem: They all use fault dimensions in km rather than normalizing fault dimensions to fault length.

Checking the non-normalization of fault dimension for Rowshandel model comparing long strike-slip fault models ss4 (M7.5) and ss7 (M7.8).

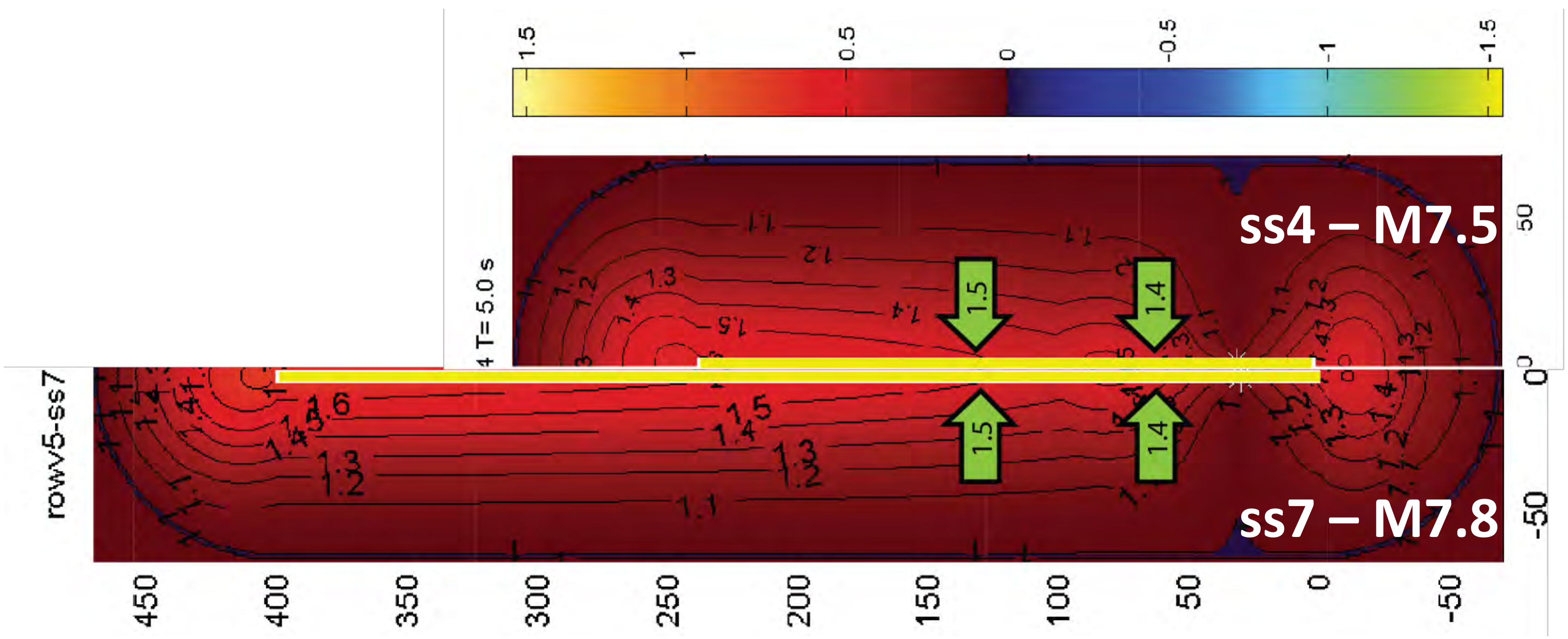

Checking the non-normalization of fault dimension for Spudich and Chiou model comparing long strike-slip fault models ss4 (M7.5) and ss7 (M7.8).

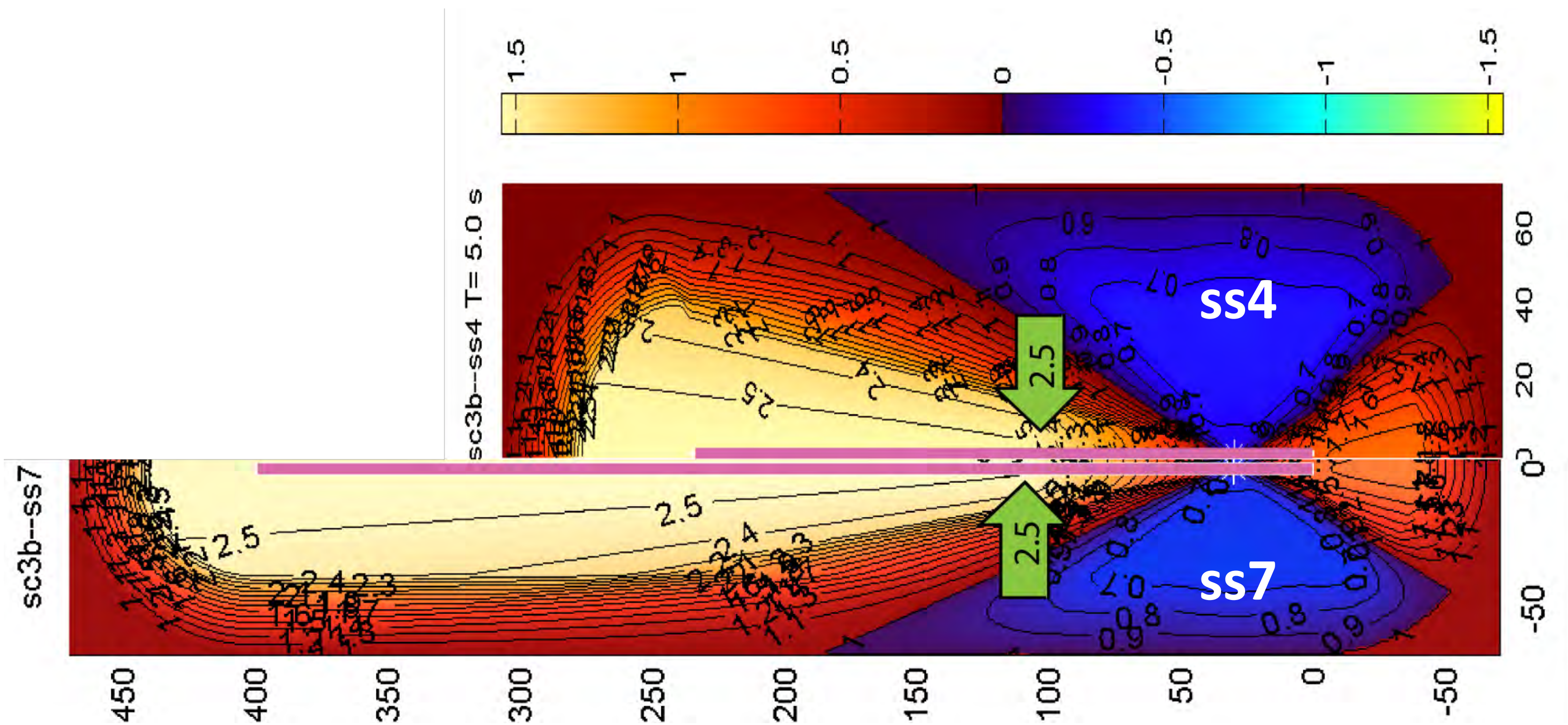

Checking the non-normalization of fault dimension for Shahi and Baker model comparing long strike-slip fault models ss4 (M7.5) and ss7 (M7.8).

Note that CBSB/CBR is shown – not absolute amplitudes

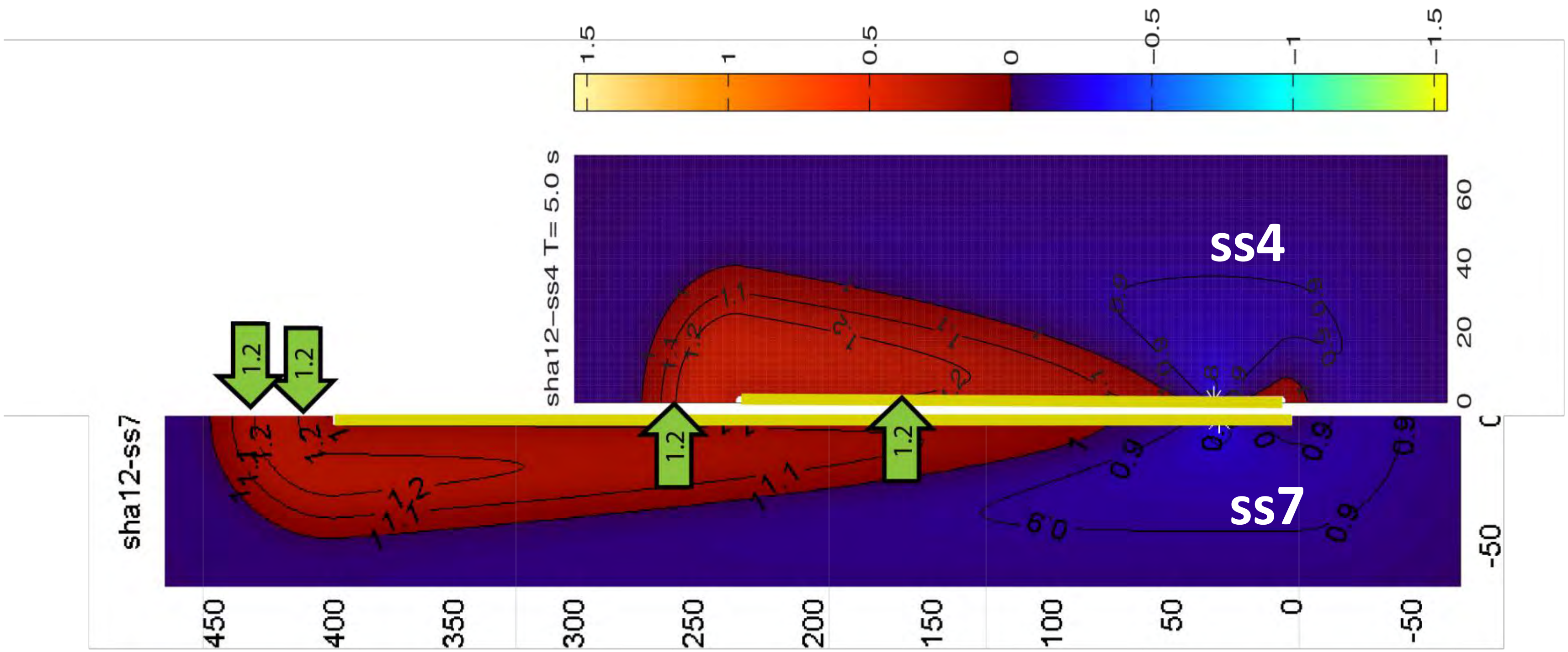

Comparison of predicted directivity from models sha12, sc3b, and row12 for M7.0 shallowly-dipping reverse fault test model rv4

sha12 has a uniform high amplitude zone over the fault trace.
row12 has strong directivity to the NW, caused by the length of the rupture path from the hypocenter to the NW corner of the fault.
Sc3b has a high amplitude zone just updip from the hypocenter, caused by the point source radiation pattern.

Shahi and Baker | Spudich and Chiou (model 3) | Rowshandel

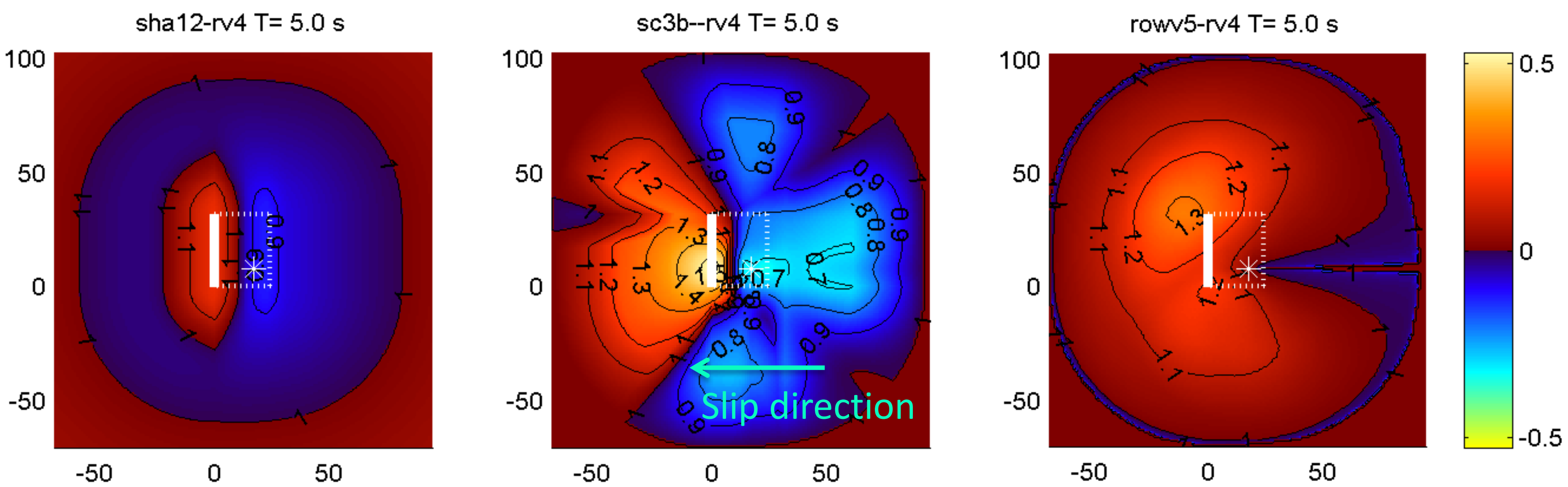

Comparison of predicted directivity from models sha12, sc3b, and row12 for M7.0 shallowly-dipping oblique-slip test model ro6.

The effect of rake rotation is more apparent in reverse faulting earthquake ro6, which had a 135° rake.

Shahi and Baker

Spudich and Chiou (model 3)

Rowshandel

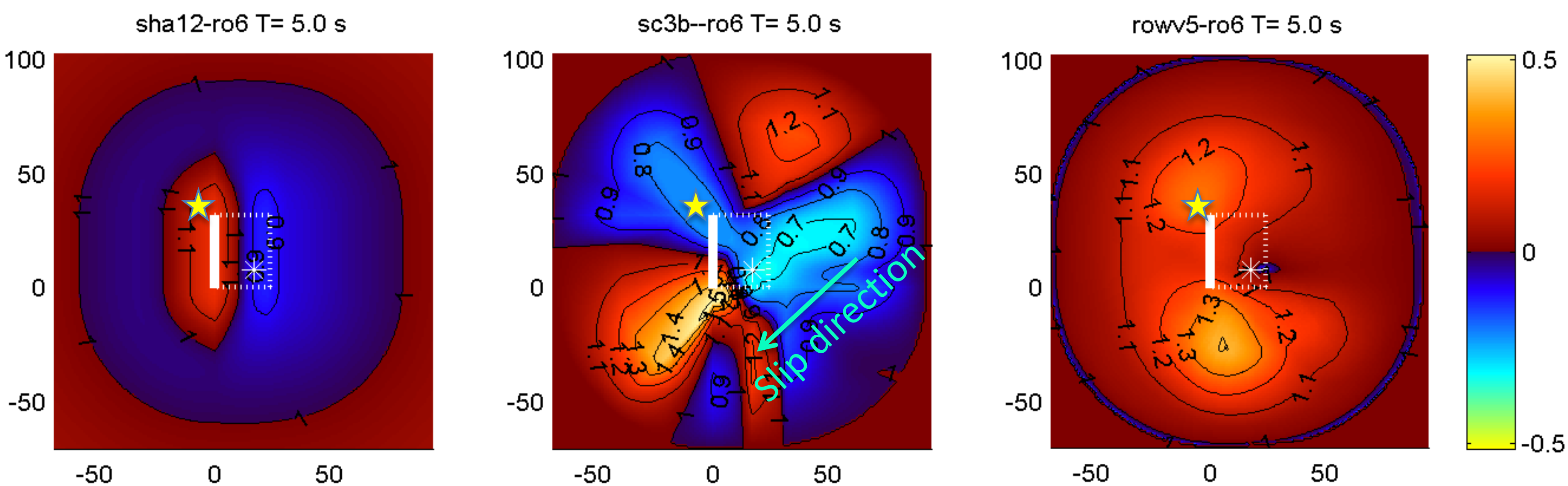

NOTE the disagreement in the directivity prediction at the site indicated by a yellow star.

Comparison of four directivity models for rv7

M7.5 45dg bend

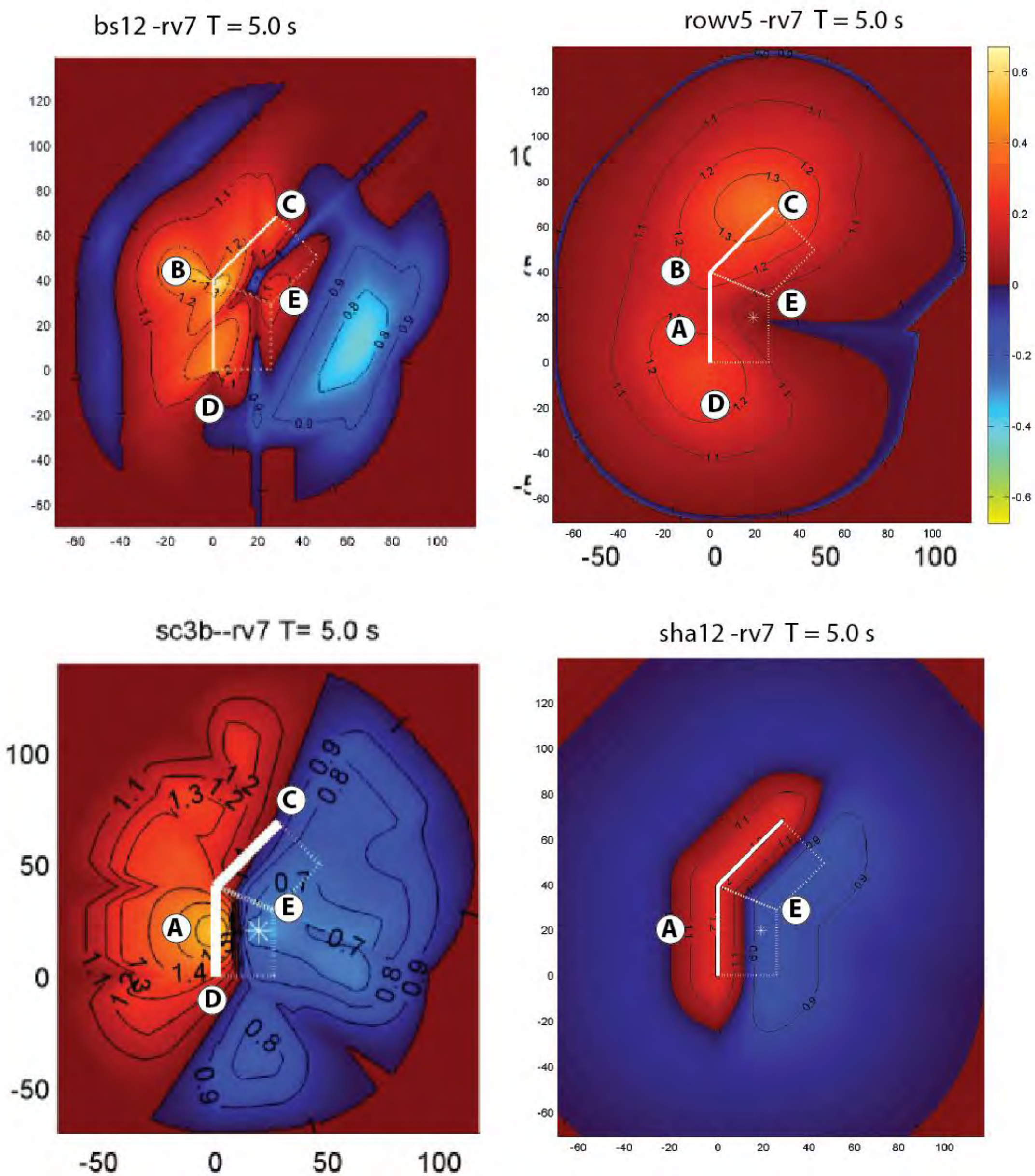

This model makes clear that at least for reverse faults, the assumptions of the directivity models have a stronger effect on the predictions than do the data

Comparison of Rowshandel, Shahi and Baker, and Spudich and Chiou for ChiChi and Denali

Directivity amplification factor for 1999 Chi-Chi Taiwan earthquake, for three proposed directivity models at 5s period.

Shahi and Baker

Spudich and Chiou (model 3)

Rowshandel

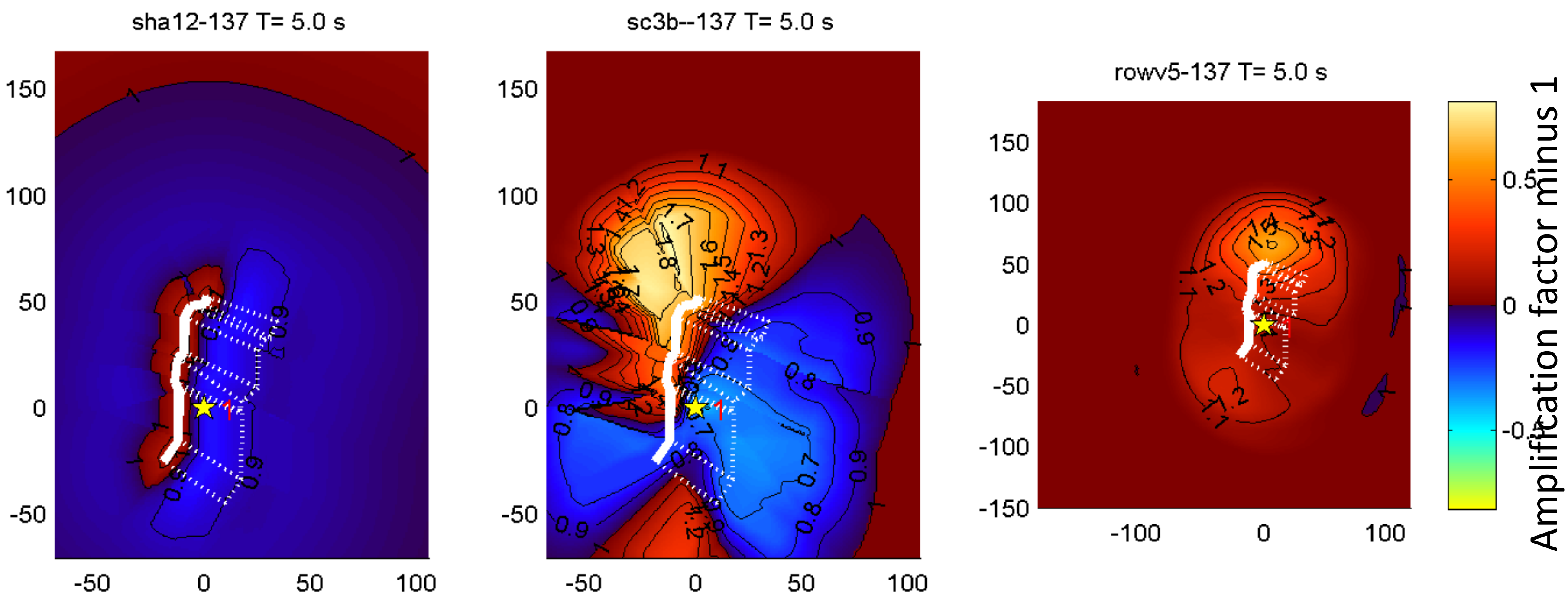

Absolute amplitudes likely to change; compare only spatial pattern

Colors show amplification factor, contours are amp factor minus 1

Directivity amplification factor for 1999 Chi-Chi Taiwan earthquake, for three proposed directivity models at 5s period.

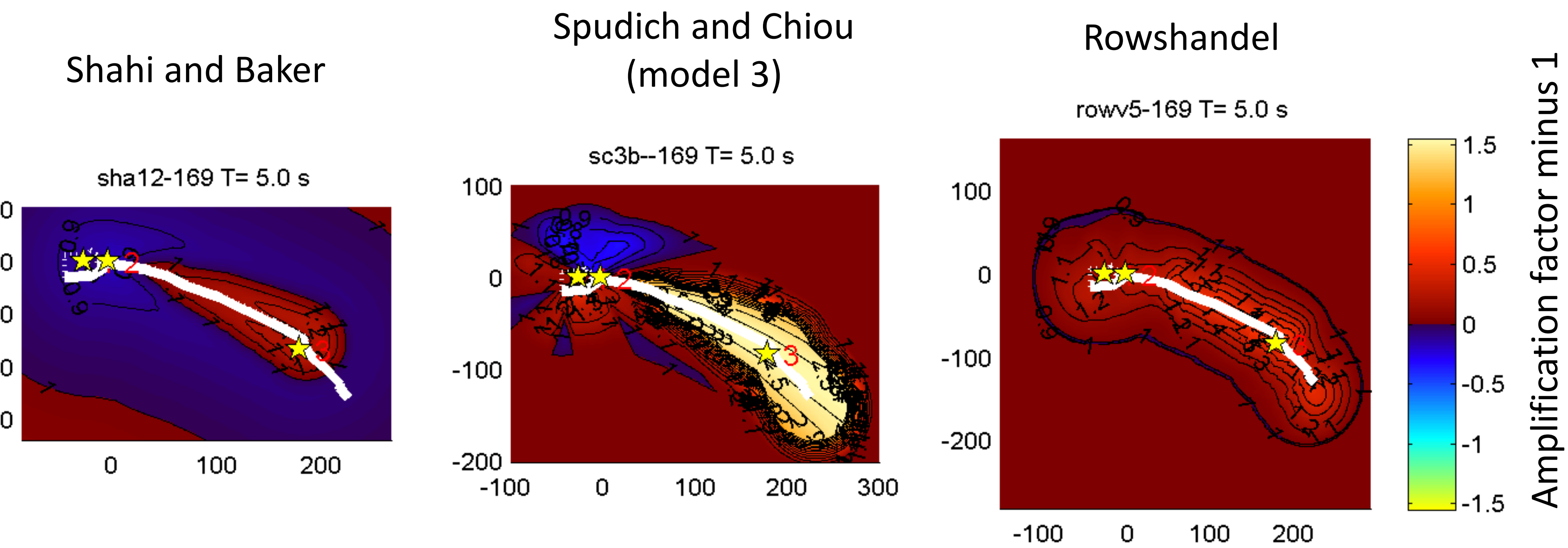

Absolute amplitudes likely to change; compare only spatial pattern

Colors show amplification factor, contours are amp factor minus 1

M7.9 Denali Earthquake, Shahi and Baker pulse directivity model

Amplification factor (CBSB/CBR) for 5 s SA shown

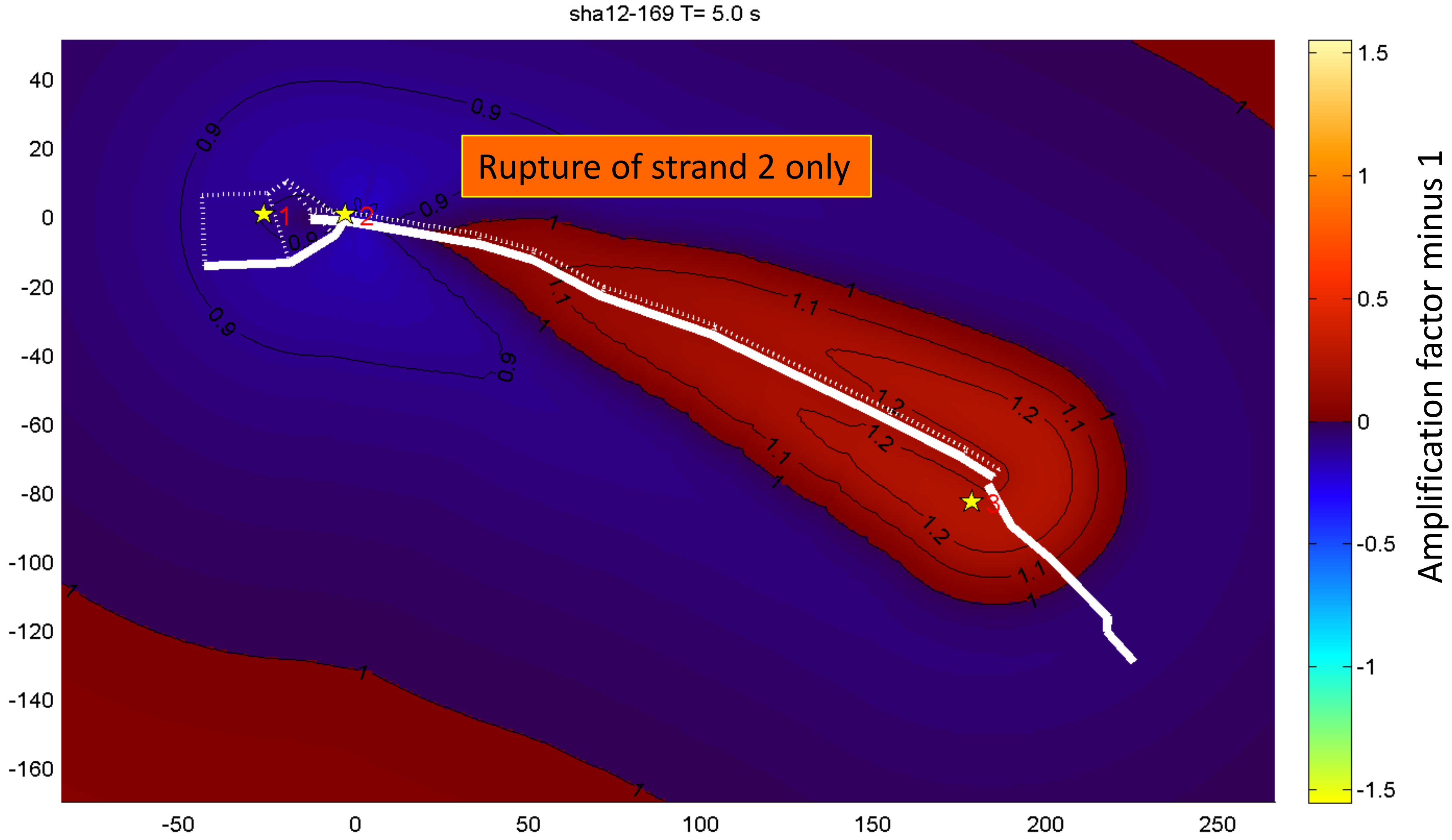

M7.9 Denali Earthquake, Spudich & Chiou IDP model 3

Amplification factor for 5 s SA shown

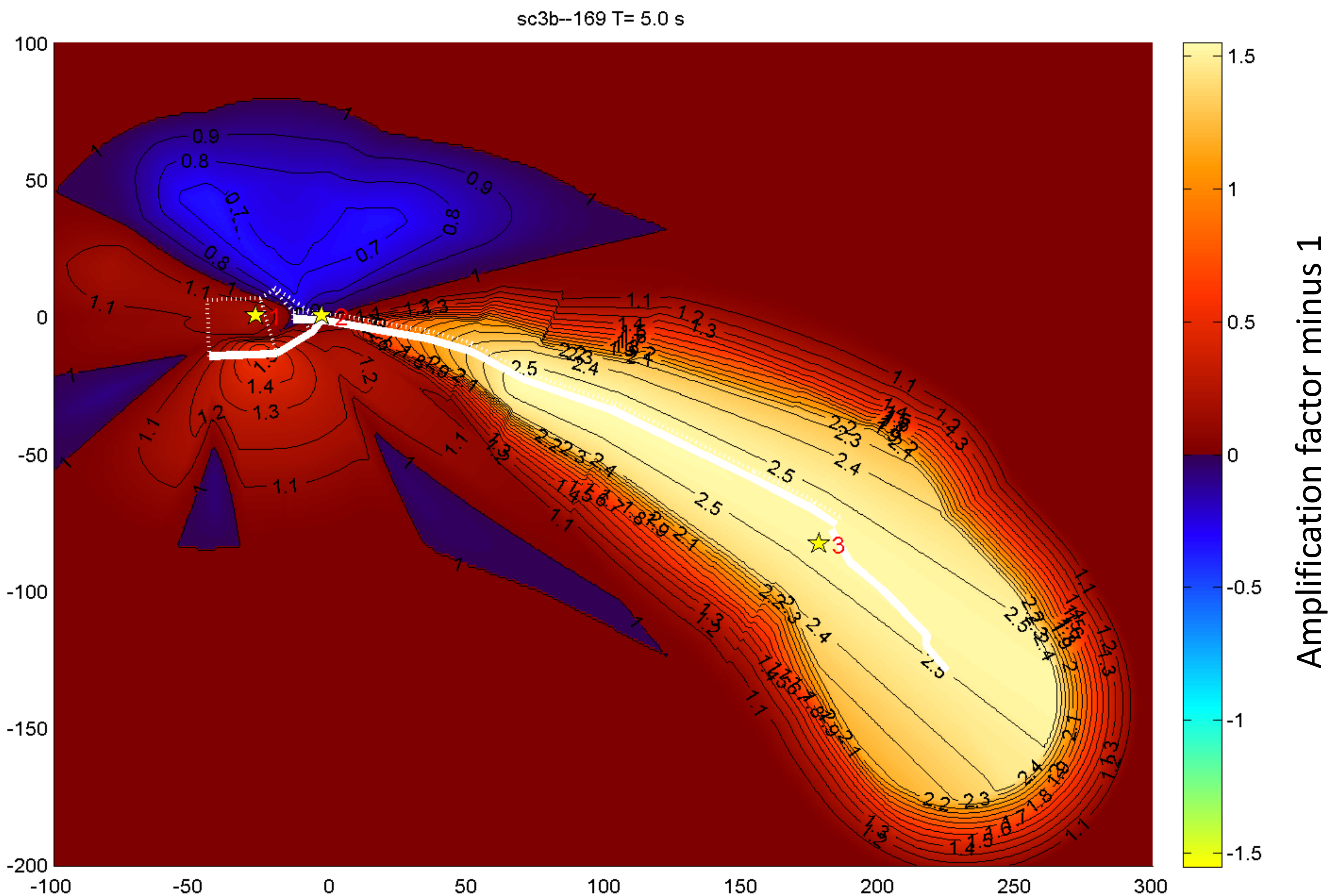

M7.9 Denali Earthquake, Rowshandel model

Amplification factor for 5 s SA shown

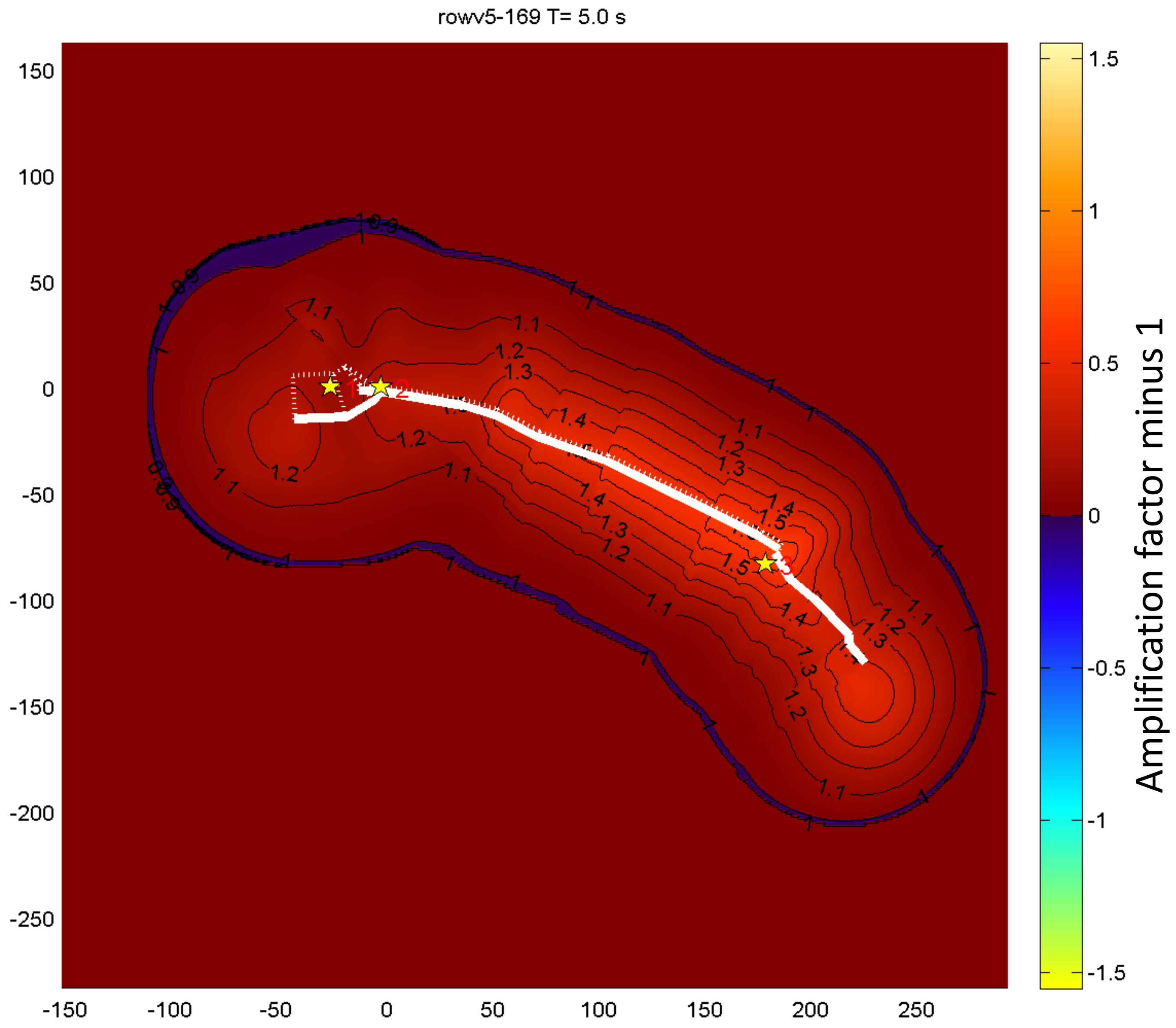

M7.6 Chichi Earthquake, Shahi and Baker pulse model

Amplification factor for 5 s SA shown

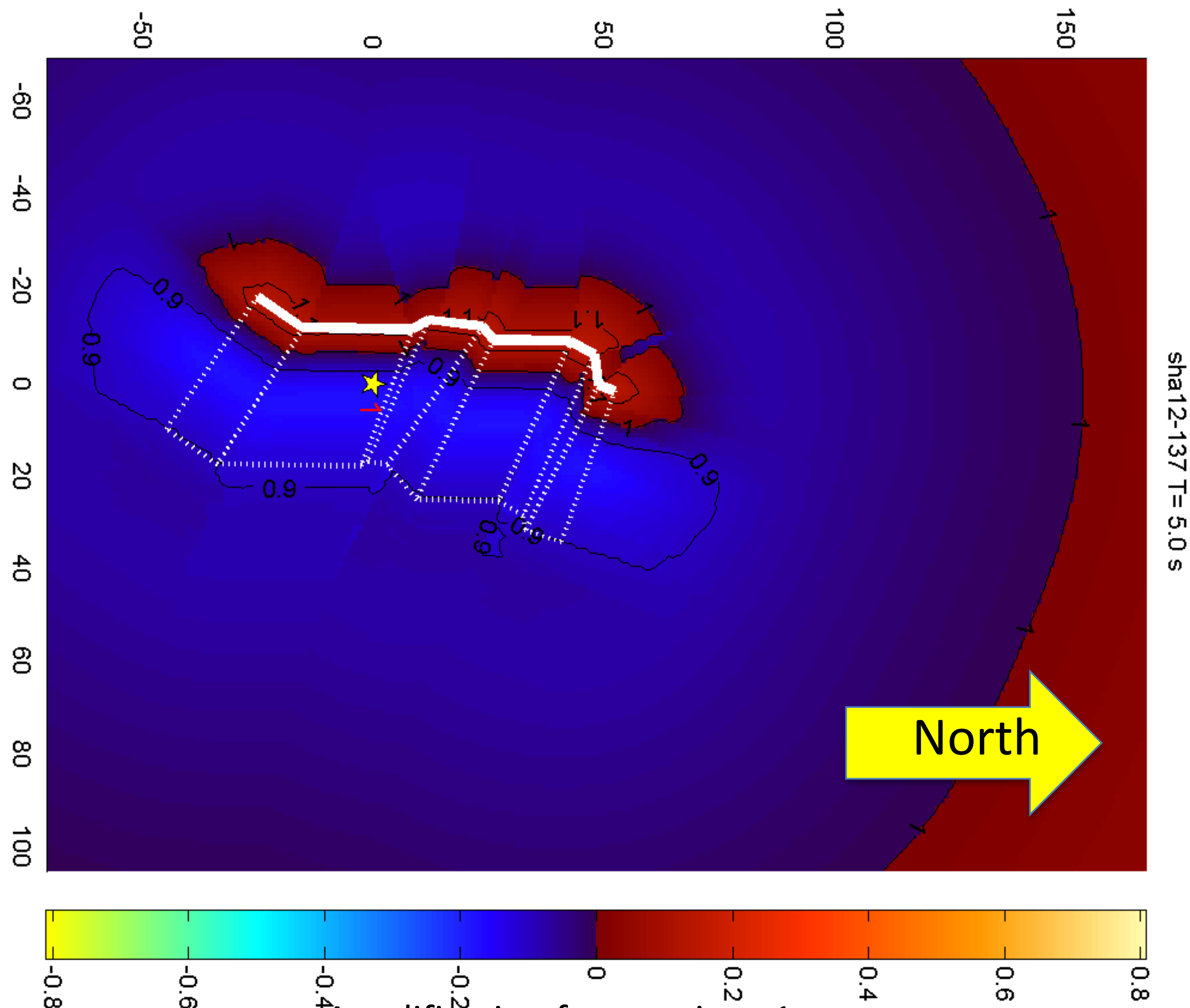

Amplification factor minus 1

M7.6 Chichi Earthquake, Spudich & Chiou IDP model 3

Amplification factor for 5 s SA shown

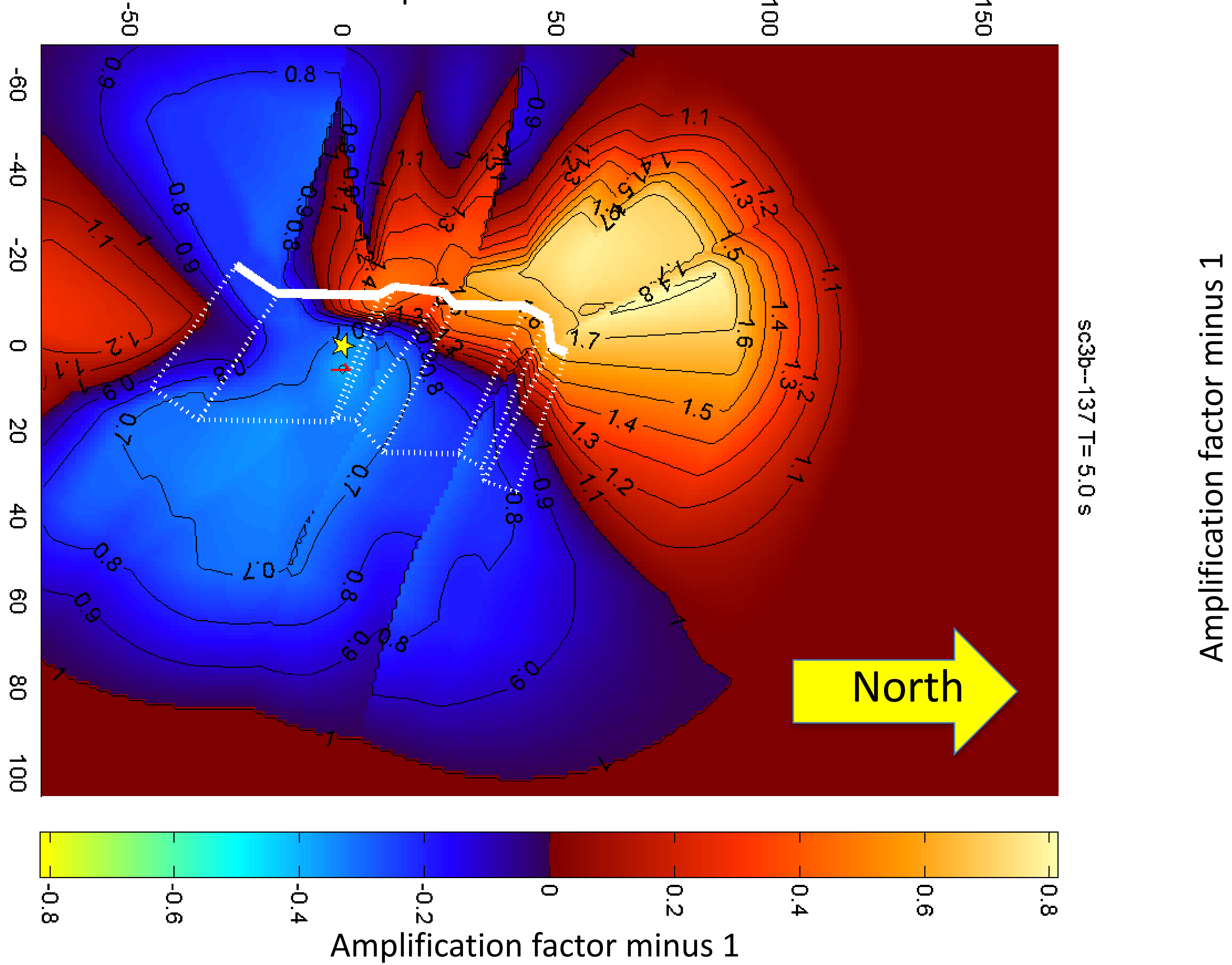

M7.6 Chichi Earthquake, Rowshandel model

Amplification factor for 5 s SA shown

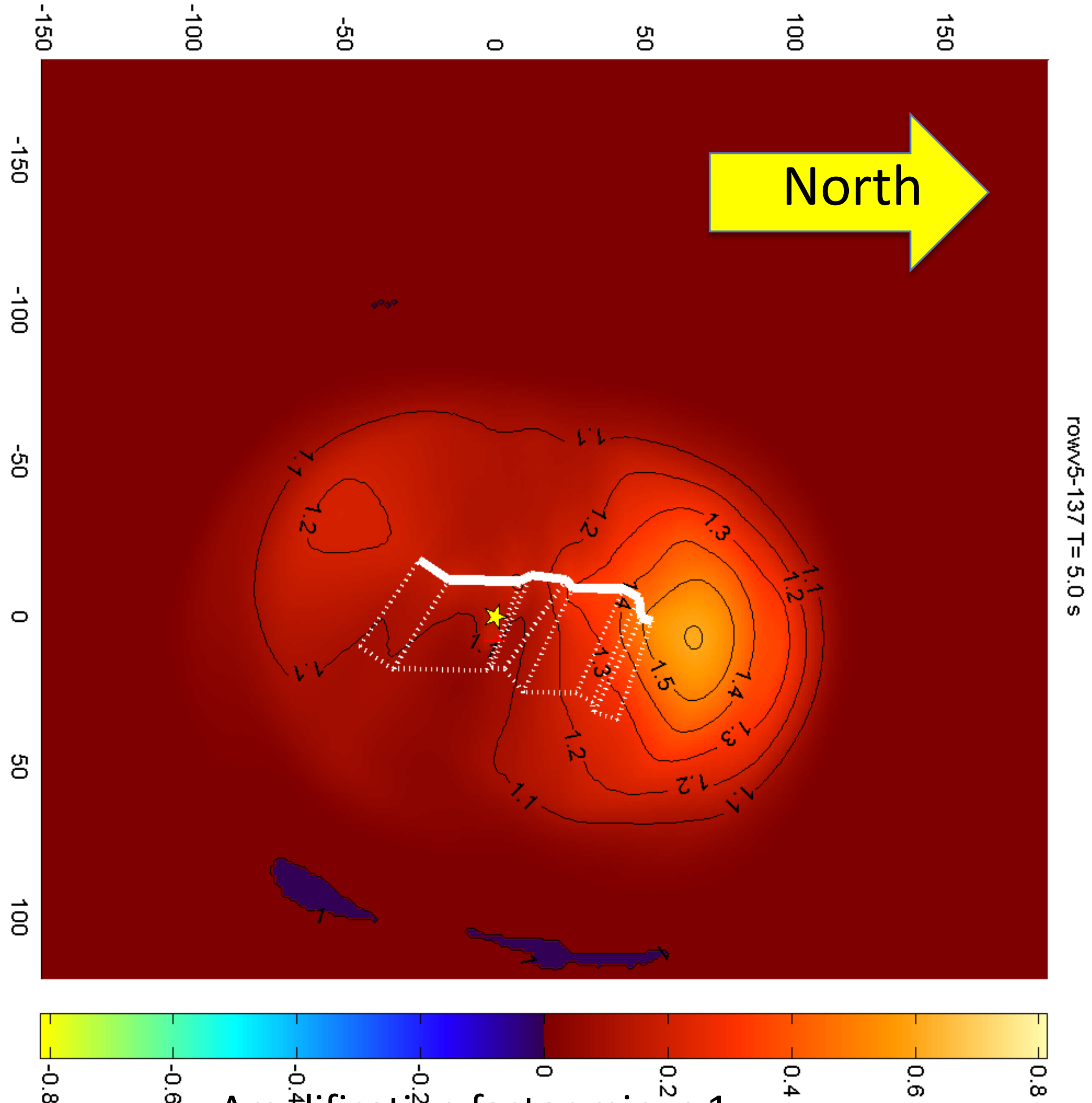

$$\left(\frac{\text{radius of magenta circle}}{\text{radius of green circle}}\right) = \left(\frac{\text{observed motion}}{\text{predicted motion}}\right)$$

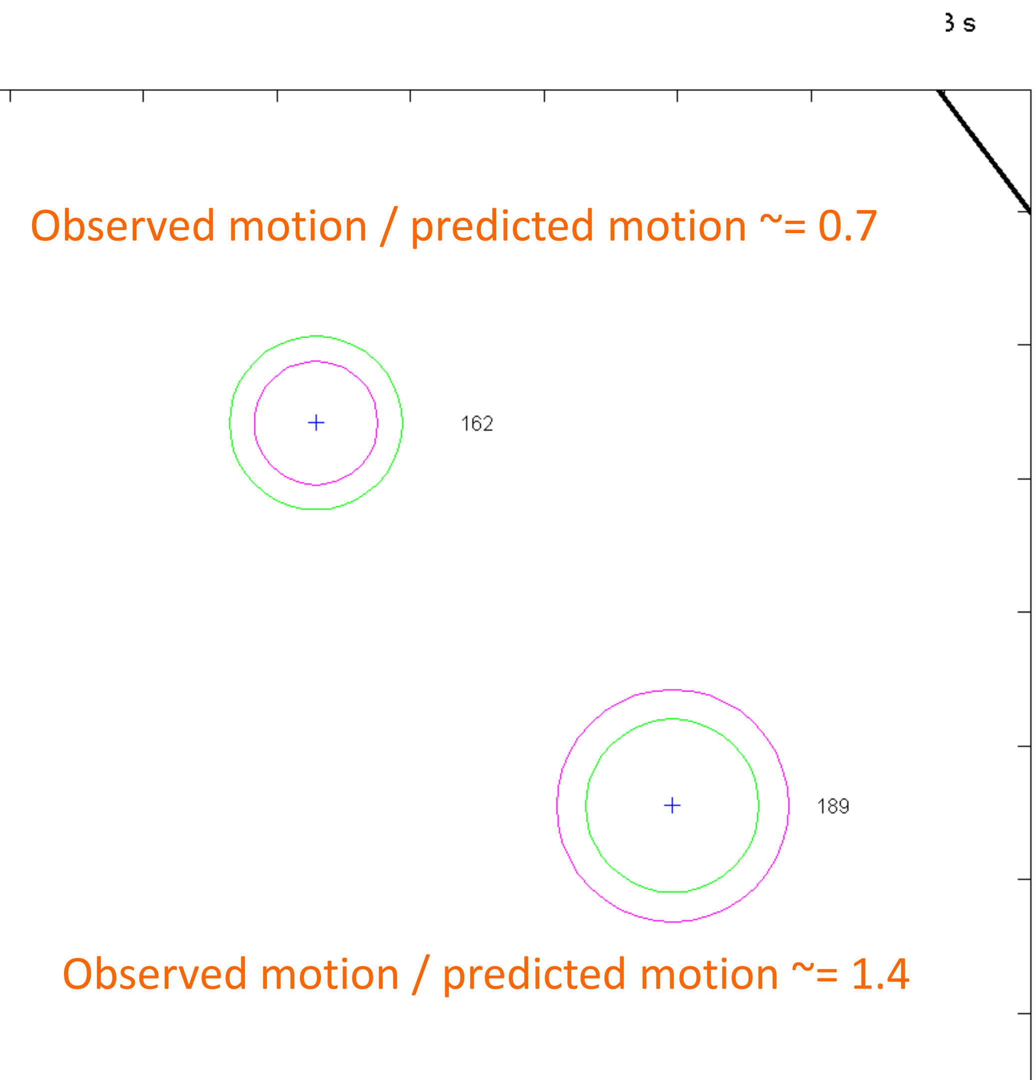

Symbol key for ground motion intraevent residual plots

$$\left(\frac{\text{radius of magenta circle}}{\text{radius of green circle}}\right) = \left(\frac{\text{observed motion}}{\text{predicted motion}}\right)$$

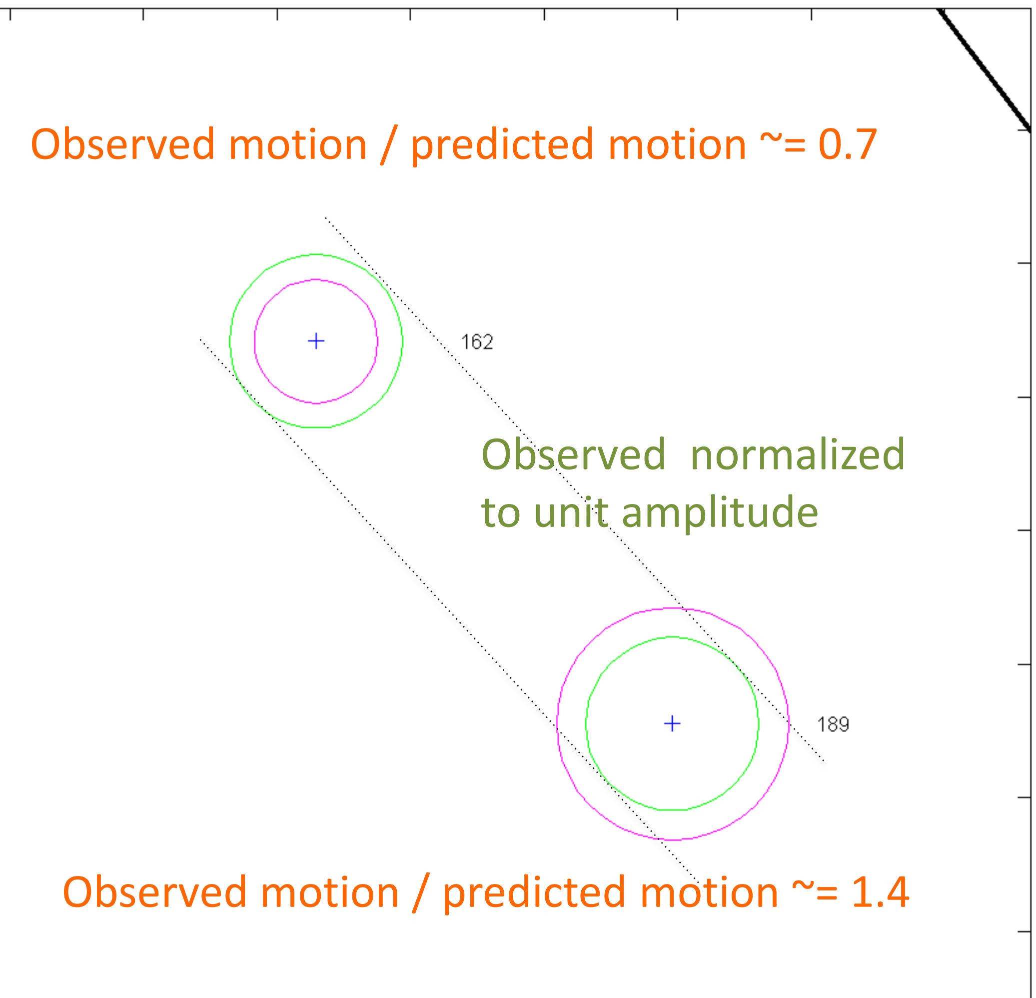

Symbol key for ground motion interevent residual plots

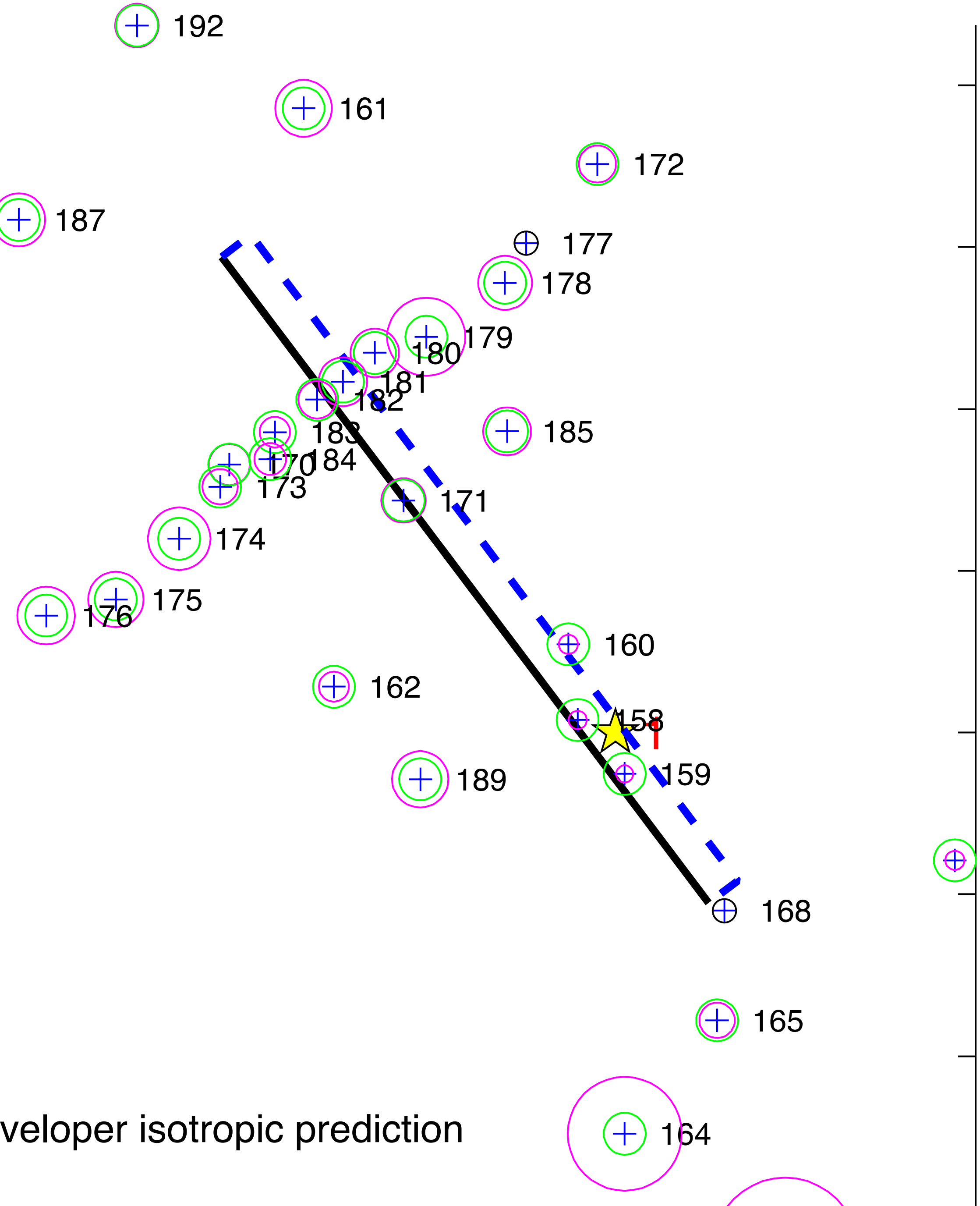

Map of intra-event residuals of gmroti50 at 3s from Campbell and Bozorgnia (2008) for the 1979 Imperial Valley earthquake

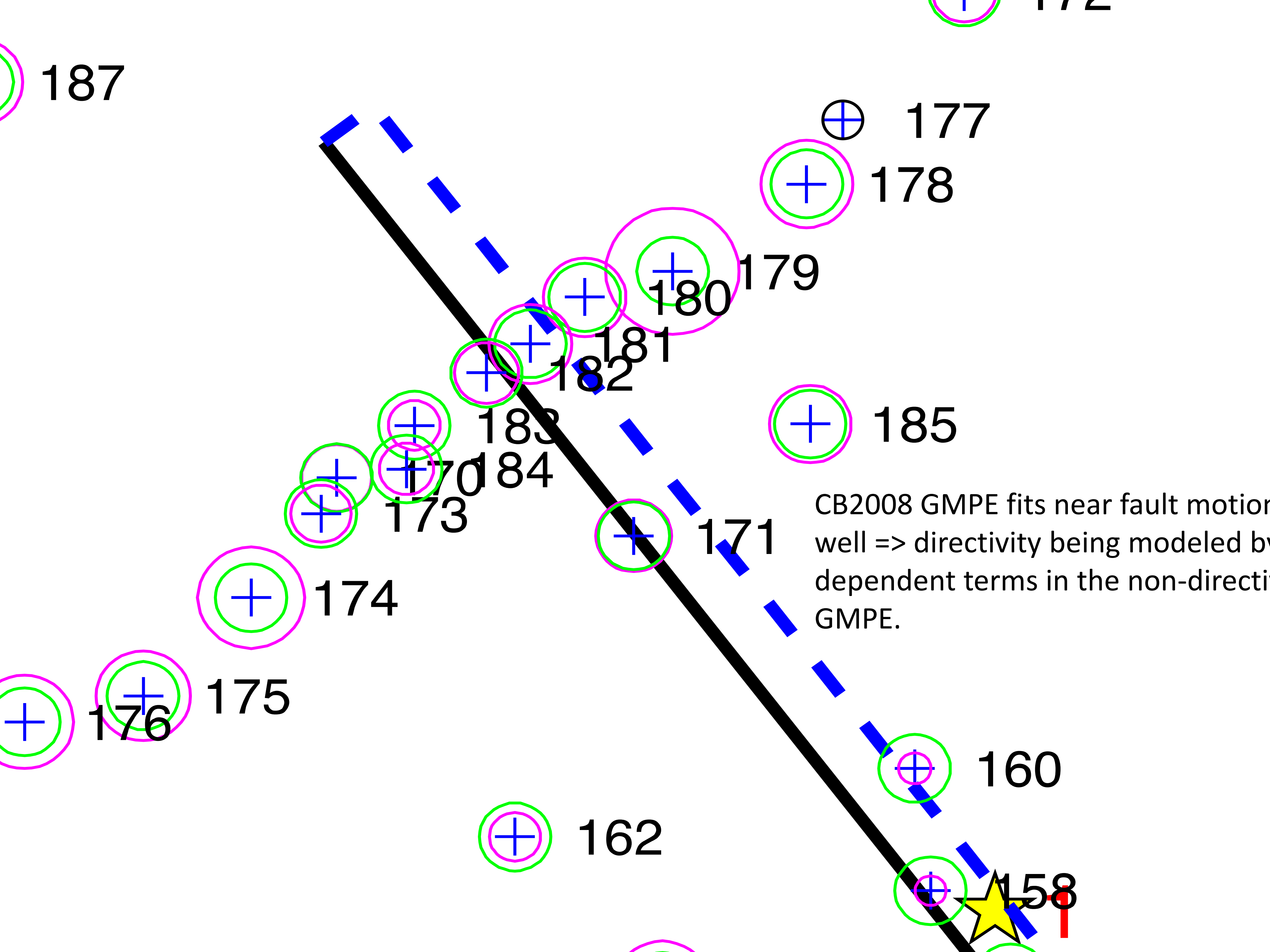
187
177
178
179
180
181
182
183
170
184
173
171
185
174
175
176
160
162
158
CB2008 GMPE fits near fault motion
well => directivity being modeled b
dependent terms in the non-directi
GMPE.

Bayless and Somerville

Overview

- Fits residuals of the NGA predicted GMRotI50 spectral accelerations relative to Fault Normal (FN), fault parallel (FP) and 50th percentile (RotD50) components for 4 of the NGA GMPEs individually.

- Separate treatment of strike-slip and dip-slip faults

- Uses the Somerville et al. 1997 predictors with some simple modifications, thus maintains simple formulation based on fault and rupture geometry

- Combined results of the 4 NGA form a generic directivity correction model

- Formulation is simple enough to be applied to existing GMPEs to provide correction for directivity

Major Changes from Somerville et al 1997 Model

1. Absolute scaling with fault dimensions

- Replaced parameter "X" with "s" – the length of the fault between the epicenter and site rupturing towards the site. There is no upper bound on s.
- This removes "normalized" characteristic of the model and allows for extrapolation to larger faults
- Also addresses the inconsistency of f_D predictions for :

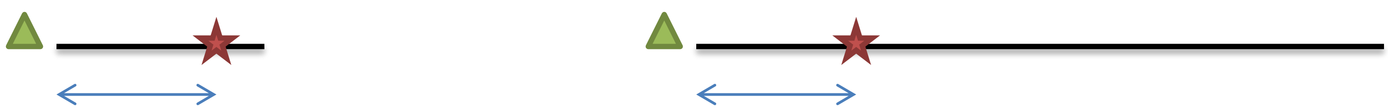

large X on a small fault vs. small X on a large fault.

(10 km, large X) (10 km, small X)

Major Changes from Somerville et al 1997 Model (cont.)

2.Distance, Magnitude, and Azimuthal Tapers

- Reduce predictor to zero outside defined range
- Removes the previous ‘excluded zone’ with its abrupt edges

3.Introduces some guidance about how to handle oblique slip earthquakes and geometrically complicated quakes

URS

Equations

Used to be X

Used to be ∪.
2∪ αγρεεσ ωιτη ραδιατιον πατερν

For Strike-Slip:

Geometric Directivity Predictor:	$f_{geom}(s,\theta) = \log_e(s) * (0.5\cos(2\theta) + 0.5)$	
Distance Taper:	$T_{CD}(R_{rup}, L) = 1$ $= 1 - (R_{rup}/L - 0.5)\ /0.5$ $= 0$	$for\ R_{rup}/L < 0.5$ $for\ 0.5 < R_{rup}/\ L < 1.0$ $for\ R_{rup}/L > 1.0$
Magnitude Taper:	$T_{M_w}(M_w) = 1$ $= 1 - (6.5 - M_w)\ /1.5$ $= 0$	$for\ M_w > 6.5$ $for\ 5.0 < M_w < 6.5$ $for\ M_w < 5.0$
Azimuth Taper:	$T_{Az}(Az) = 1$	

Equations

Used
to be Y

For Dip-Slip:

Geometric Directivity Predictor:	$f_{geom}(d, R_X) = \log_e(d) * \cos(R_x/W)$
Distance Taper:	$T_{CD}(R_{rup}, W) = 1 \quad for\ R_{rup}/W < 1.5$ $= 1 - (R_{rup}/W - 1.5)/0.5 \quad for\ 1.5 < R_{rup}/W < 2.0$ $= 0 \quad for\ R_{rup}/W > 2.0$
Magnitude Taper:	$T_{M_w}(M_w) = 1 \quad for\ M_w > 6.5$ $= 1 - (6.5 - M_w)/1.5 \quad for\ 5.0 < M_w < 6.5$ $= 0 \quad for\ M_w < 5.0$
Azimuth Taper:	$T_{Az}(Az) = \sin(\lvert Az \rvert)^2$

Rowshandel Model

Somerville et al. (1997)'s insight was that directivity is max when the

- direction of rupture advance
  aligns with the
- direction of slip and the
- direction to the observation site.

Rowshandel parameter is an integral of two dot products over the fault surface

$$x = \frac{1}{2}\frac{\sum \hat{q}\times\hat{p}}{Area}dA + \frac{1}{2}\frac{\sum \hat{q}\times\hat{s}}{Area}dA = \frac{1}{2}\frac{\sum \hat{q}\times\hat{p}}{N} + \frac{1}{2}\frac{\sum \hat{q}\times\hat{s}}{N}$$

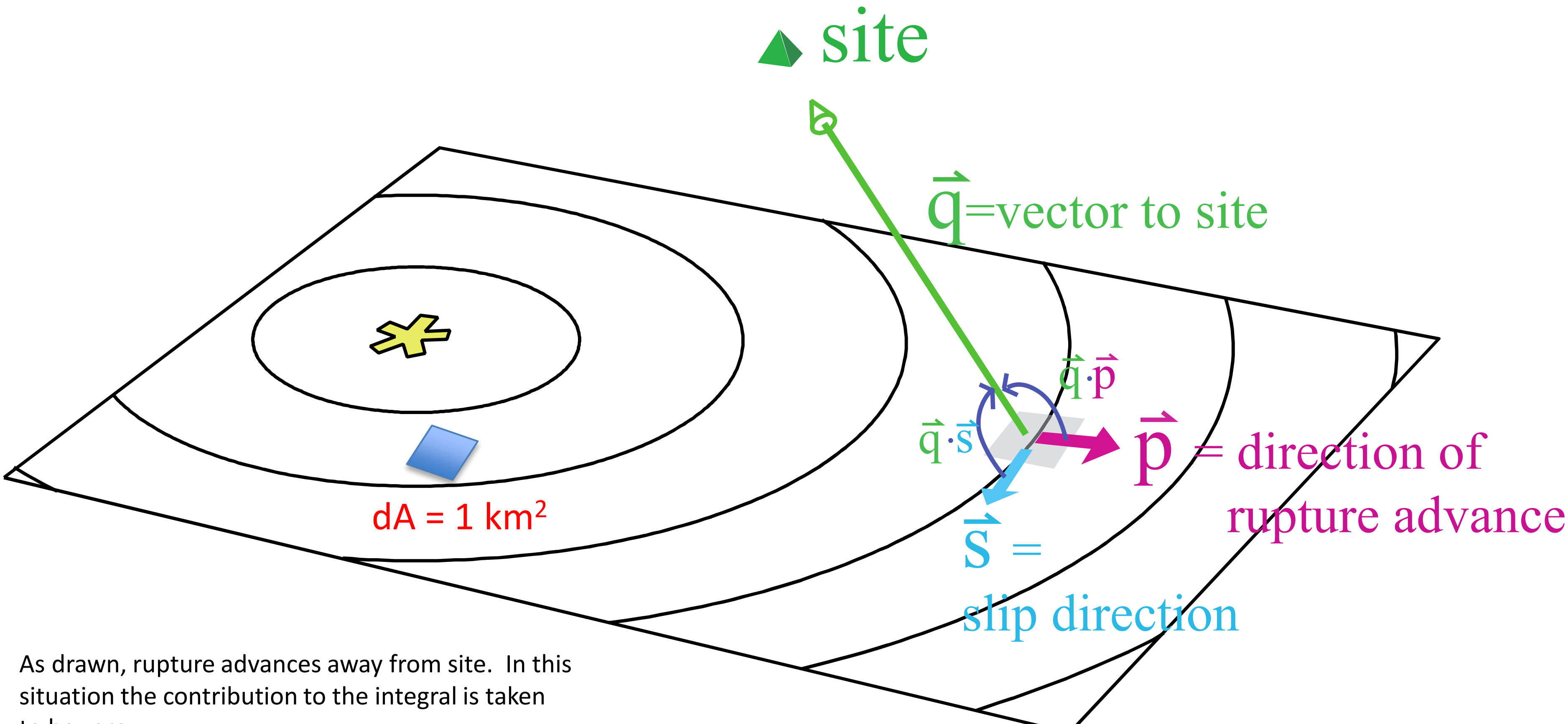

As drawn, rupture advances away from site. In this situation the contribution to the integral is taken to be zero.

New Rowshandel model is not normalized to fault length

Original Functional Form (2006, 2010)

$\ln(Y) = f(M,R,\ldots) + C\xi$ ξ : Directivity Parameter

C: Directivity Coefficient

Revised Functional Form:

$\ln(Y)=f(M,R,\ldots)+C\,\xi\,\{\ln(Lr)/\ln(Lr\text{-}max)\}$

$=f(M,R,\ldots)+C1\,\xi`$

$\xi` = \xi\,\{\ln(Lr)/\ln(Lr\text{-}max)\}$

where: Lr is the "effective rupture length" for the site

Lr-max= Lr corresponding to Mmax (~400km for M8.5)

Modification to account for fault width

Lr → √ (Lr * Lr + W’ *W’)

W’ : The portion of fault width rupturing updip (km)

Directivity saturates for high values of ξ

for $x \leq 0.5$ x not changed

for $0.5 < x < 1$ x ® $\frac{1}{2} + \frac{1}{2}\left(x - \frac{1}{2}\right)$

ASPECTS OF ROWSHANDEL MODEL

Summation over fault surface means predicted directivity amplification is spatially smoother than in models using the closest point on the rupture.

Extension to geometrically complicated faults straightforward

Non-normalized length yields a reasonable scaling for very long faults

Directivity saturates for large values of predictor

Parameter is an integral over the fault surface, means one more loop must be added to hazard codes.

Shahi and Baker model

Note –

Shahi and Baker's model is actually a model of the SA of a ground motion **pulse**, which tends to be correlated with directivity but is not what the other modelers have been modeling.

Some non-impulsive motions are amplified by directivity. These are not predicted by the Shahi and Baker model.

They categorized all records in the NGA-West2 database as not impulsive or impulsive ($I_{directivity}$=0/1), and identified pulse period *Tp*

x *pulse*

Example from 1979
Imperial Valley earthquake

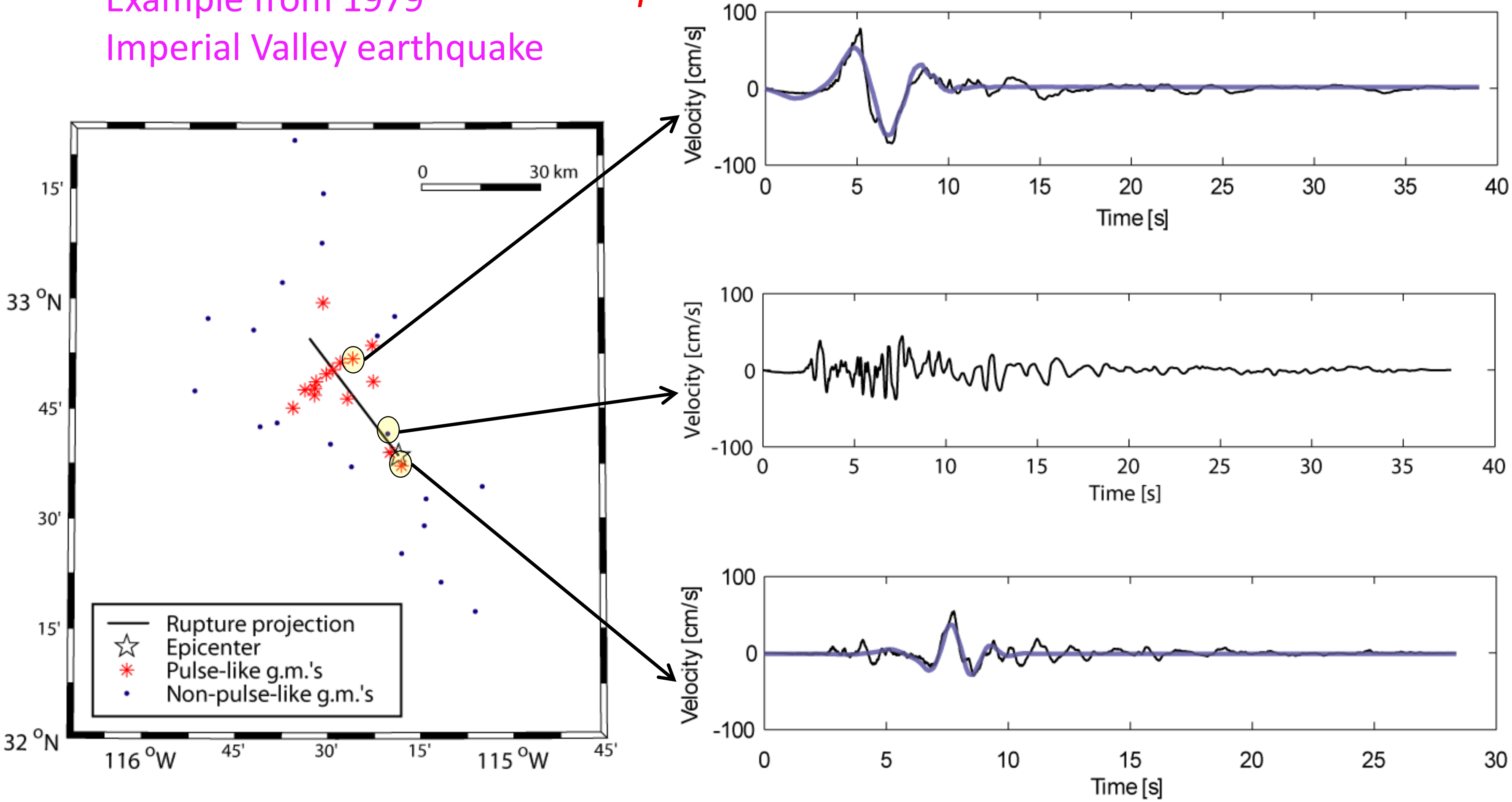

The algorithm identifies ground motions with clear pulses, and the identified motions are generally from locations where directivity is expected

Directivity ground-motion models

X *pulse*

- Ground motion models fitted
  - (CBR) Campbell Bozorgnia functional form Refitted with NGA-West2 data
  - (CBSB) Campbell Bozorgnia with Shahi & Baker directivity modifications

- The CBSB model uses the CB08 functional form as base

$$lnSa_{ij} = f(M_i, R_j, T, Vs30_j, \tilde{\Theta}, \ldots) + I_{directivity} \cdot lnAmp(T, T_p) + \eta_i + \epsilon_{ij}$$

X *pulse*

CB08 functional form

Directivity amplification

X *pulse*

$$lnAmp(T, T_p) = b_0 exp\left(b_1\left(ln\left(\frac{T}{T_p}\right) - b_2\right)^2\right)$$

← Gaussian function of period

Shahi and Baker model is not normalized to fault dimension

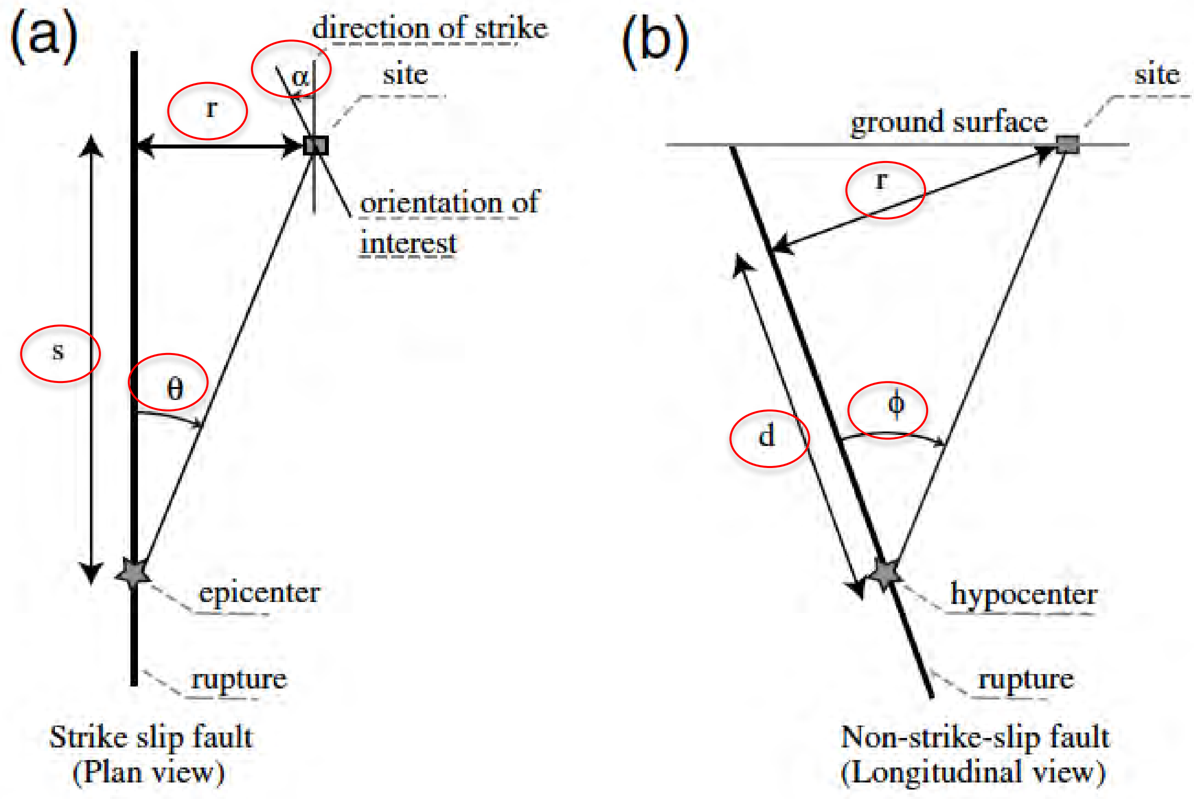

Units of s, r, d are km

From Shahi and Baker, BSSA, 2011

CBSB and CBR comparison when probability of pulse is 1

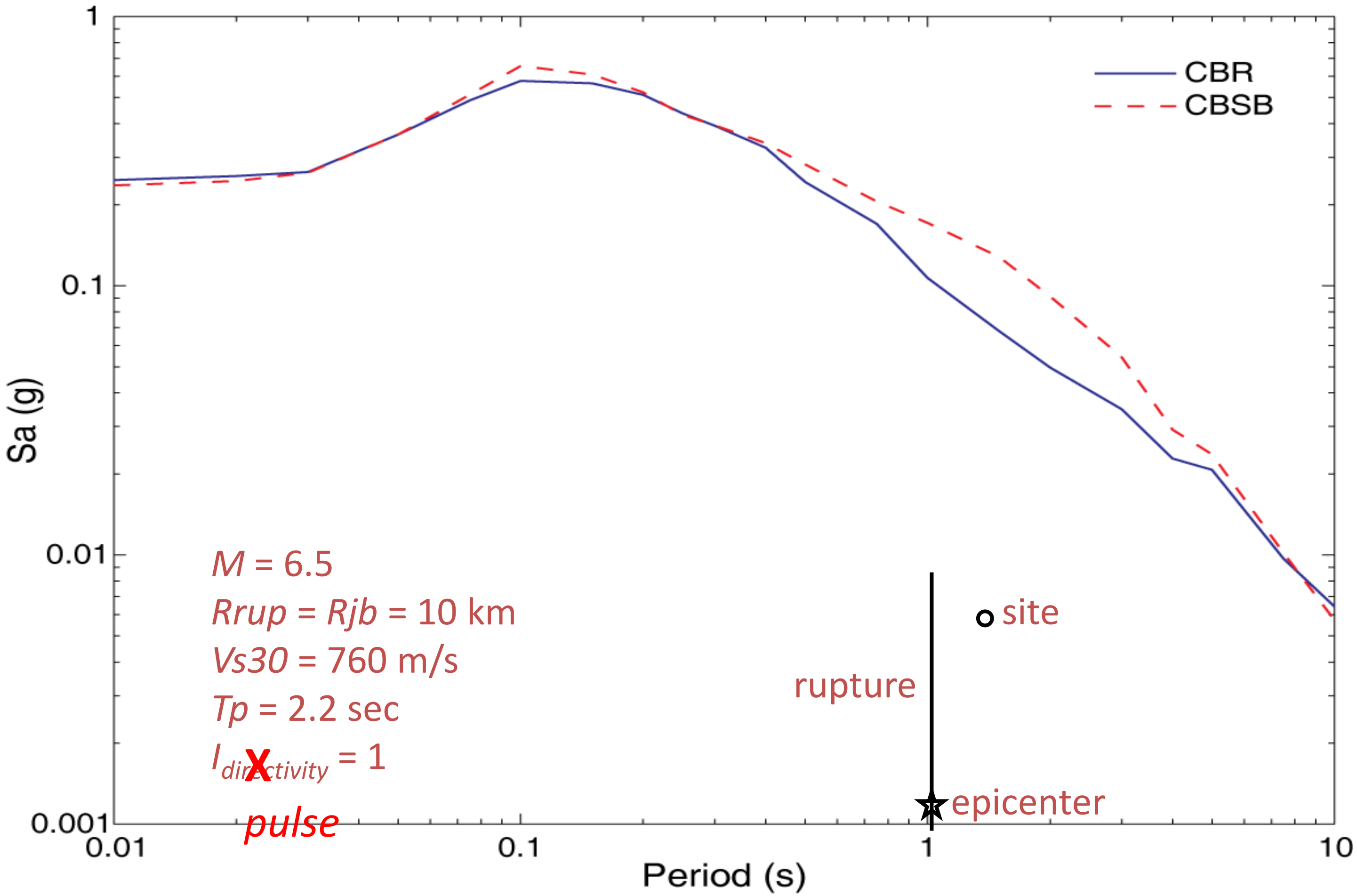

Average model

- Parameters used by directivity models are not always known (or are hard to use)

  x *pulse*

- Dropping directivity terms may lead to biased predictions of response spectra

- Proposed solution : use average directivity conditioned on *M*, *R*, *T* and averaged over hypocenters to get unbiased prediction

$$lnSa = f(M, R, T, Vs30, \ldots) + \begin{cases} I_{directivity} \cdot lnAmp(T, T_p) & \text{if } I_{directivity} \text{ and } T_p \text{ are known} \\ \mu_{lnAmp|M,R,T,\ldots} & \text{if } I_{directivity} \text{ and } T_p \text{ are unknown} \end{cases}$$

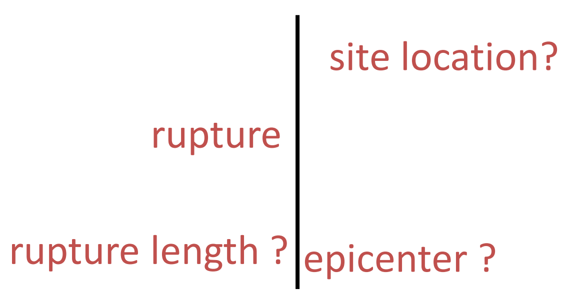

Spudich and Chiou IDP model

What’s new in the Spudich and Chiou model of directivity?

Major change: it is now a narrow-band model. Directivity is max at a period that increases with magnitude

We have found a simpler expression for the much-maligned radiation pattern term.

We have an improved algorithm for calculating distance D along the fault from hypocenter to closest point.

No change: It was and still is a non-normalized model!

Fitting AS residuals by *a+b*IDP* for each quake and period seems to show a magnitude-dependent period *Tmax* of the peak slope *bmax*

Red circle indicates period having the largest slope *b*

Below M 6 the biggest b values occur at shorter periods.

Above M 7 the biggest b values occur at longer periods.

Magnitude increases

Circle radius proportional to slope b

b > 0 = white or red, b < 0 = black filled

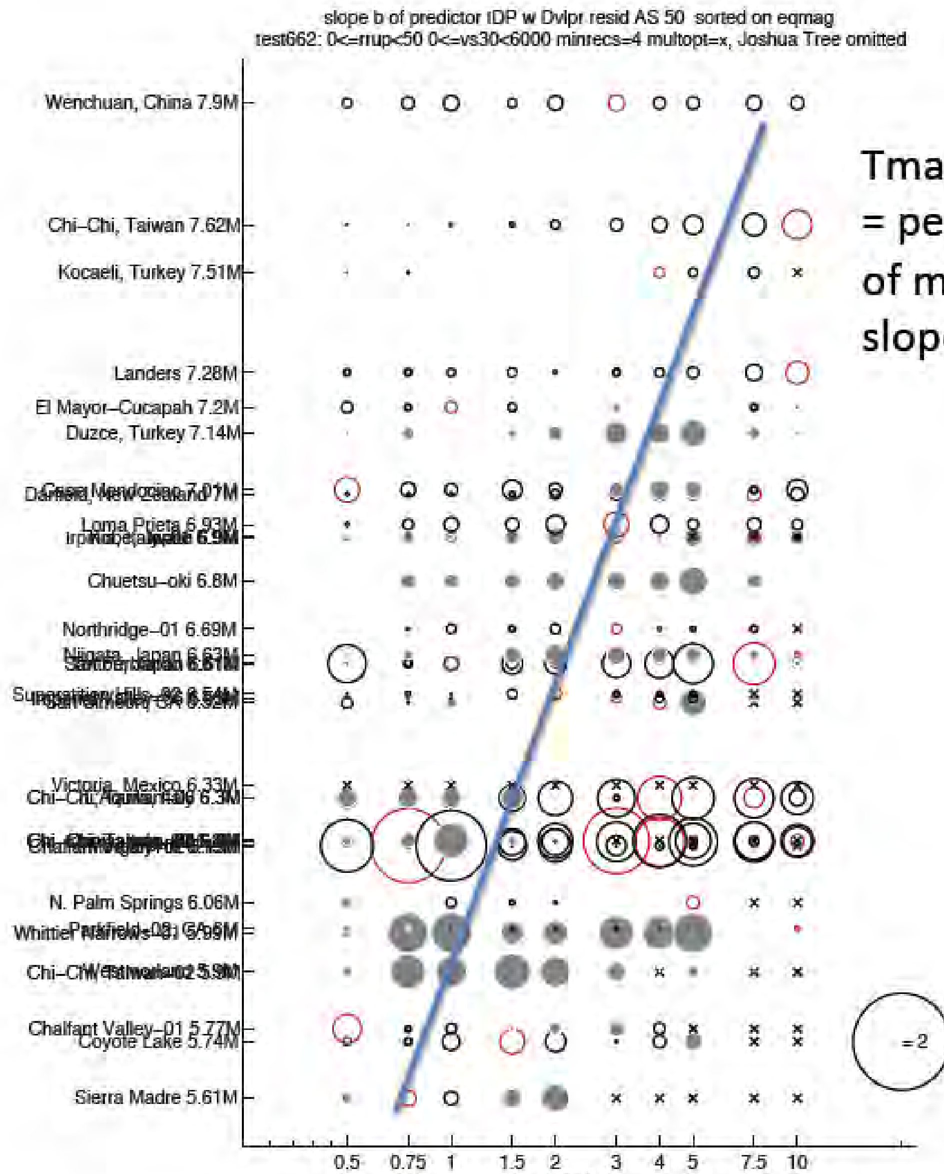

Tmax(M) = period of max b-slope

Spudich and Chiou new functional form

$$\hat{f}_D = f_r(R_{rup})\ b(M,T)\ \left(IDP - \overline{IDP}(R_{rup})\right)$$

$$b(\boldsymbol{M},T) = \left(c_2 + c_3\, max(\boldsymbol{M} - c_1\,, 0)\right) exp[q(\boldsymbol{M},T)]$$

$$q(\boldsymbol{M},T) = -[log_{10}T - (c_4 + c_5\boldsymbol{M})]^2/2s^2$$

M and *T* are moment-magnitude and oscillator period.
c_1, c_2, c_3, c_4, c_5, and *s* are period-independent constants.
fr is a distance taper that linearly tapers to
IDP(Rrup) is the average value of the *IDP* along the Rrup racetrack.

REFERENCES

Abrahamson, N. (2000). Effects of rupture directivity on probabilistic seismic hazard analysis, *6th Int. Conf. on Seismic Zonation*, **Proceedings**: Earthq. Eng. Res. Inst. CD-2000-01.

Rowshandel, B. (2006). Incorporating source rupture characteristics into Ground-Motion hazard analysis models. Seismological Research Letters 77 (6), 708-722.

Rowshandel, B. (2010). Directivity correction for the Next Generation Attenuation (NGA) relations*, Earthq. Spectra*, **26:2***,* 525-559, doi 10.1193/1.3381043.

Shahi, S.K. and J.W. Baker (2011). An empirically calibrated framework for including the effects of near-fault directivity in probabilistic seismic hazard analysis. Bulletin of the Seismological Society of America 101(2), 742-755.

Somerville, P.G., Smith, N.F., Graves, R.W., and Abrahamson, N.A. (1997). Modification of empirical strong ground motion attenuation relations to include the amplitude and duration effects of rupture directivity. *Seismol. Res. Let.* **68:1**, 199-222.

Spudich, P., and Chiou, B.S.-J. (2008). Directivity in NGA earthquake ground motions: Analysis using isochrone theory. *Earthquake Spectra,* **24:1**, 279-298.

Bayless. J. and P.Somerville (2013). In *Final Report of the Directivity Working Group*, PEER report XXXX-XX, in preparation.

Rowshande (2013). In *Final Report of the Directivity Working Group*, PEER report XXXX-XX, in preparation.

Shahi , S., andJ J. Baker (2013). In *Final Report of the Directivity Working Group*, PEER report XXXX-XX, in preparation.

Spudich, P. and B. S. J. Chiou (2013). In *Final Report of the Directivity Working Group*, PEER report XXXX-XX, in preparation.

Watson-Lamprey (2013_/   (2013). In *Final Report of the Directivity Working Group*, PEER report XXXX-XX, in preparation.

THE END

NOW, ON TO NGA-WEST 3

Goals of Directivity Working Group

- To develop directivity functional forms which NGA-W2 developers can choose to include in their regressions, so that the directivity is included *ab initio* in the resulting ground motion prediction equations, instead of being an after-the-fact correction. (Solving the 'unsmoothing' and the 'masquerade' problems.)

- To develop updated/new directivity models using a more current and expansive record set than previous versions

- To correct flaws in most previous directivity models that yielded improper scaling with fault dimension, e.g. Somerville et al. (1997), Rowshandel (2006, 2010)

Nshmp slide dump

PROBLEMS IN THE 2008 NGA *post hoc* 'CORRECTION' APPROACH TO DIRECTIVITY

directivity functions were developed (e.g. Spudich and Chiou, 2008; Rowshandel 2010) as *post hoc* 'corrections' to the median of a NGA GMPE by fitting directivity functional forms to the residuals of that GMPE

The 'centering' problem:

- the average directivity effect in the observed dataset is implicitly included in the median of a 2008 NGA GMPE
- the reference directivity condition corresponding to that median motion is unclear.

The 'unsmoothing' problem:

- some GMPE developers deliberately allowed misfits to the data in order to smooth their predicted motions as functions of periods. The addition of a directivity 'correction' can undo the smoothing intended by the GMPE developers.

The 'masquerade' problem:

- Some of the directivity signal has been modeled in the 2008 GMPEs by other terms, most likely the distance dependence

- **Centering the directivity parameter.**

Following a suggestion by N. Abrahamson, the directivity term in the GMPE can be centered the following way:

$$\ln y = (usual\ GMPE) + c(T)\left(d - \bar{d}(R)\right)$$

Where

d is the directivity predictor (e.g. IDP)

$\bar{d}(R)$ is the average (or median) value of d at distance R over the footprint of the directivity function for each earthquake. Note that this value is specific to each rupture geometry.

c is an empirical coefficient

The R-dependence of directivity is carried by the GMPE, and the azimuthal dependence of directivity is in $\left(d - \bar{d}(R)\right)$

Two circumstances in which the average value of the directivity parameter is needed:

To solve for directivity coefficients in the GMPEs, the average value of directivity parameter over all stations recording each earthquake (having a finite fault model) is needed. This has been done by:

Rowshandel,
Shahi and Baker,
Spudich and Chiou

To use a new GMPE including directivity to predict motions for a hypothetical earthquake, the average directivity parameters for the target rupture geometries are needed. The user could calculate this directly for target ruptures.

Alternatively, a model for $\bar{d}(M, R, T)$ when hypocenter position is unknown has been developed by Shahi and Baker for vertical strike-slip faults .

Two NGA-West2 directivity models are explicitly ‘narrowband’ models, meaning that the directivity amplification peaks at some period that depends on the target earthquake’s M.

- Shahi and Baker
- Spudich and Chiou

Watson-Lamprey’s model is implicitly narrow-band

Compute "*Lr*" for a Site

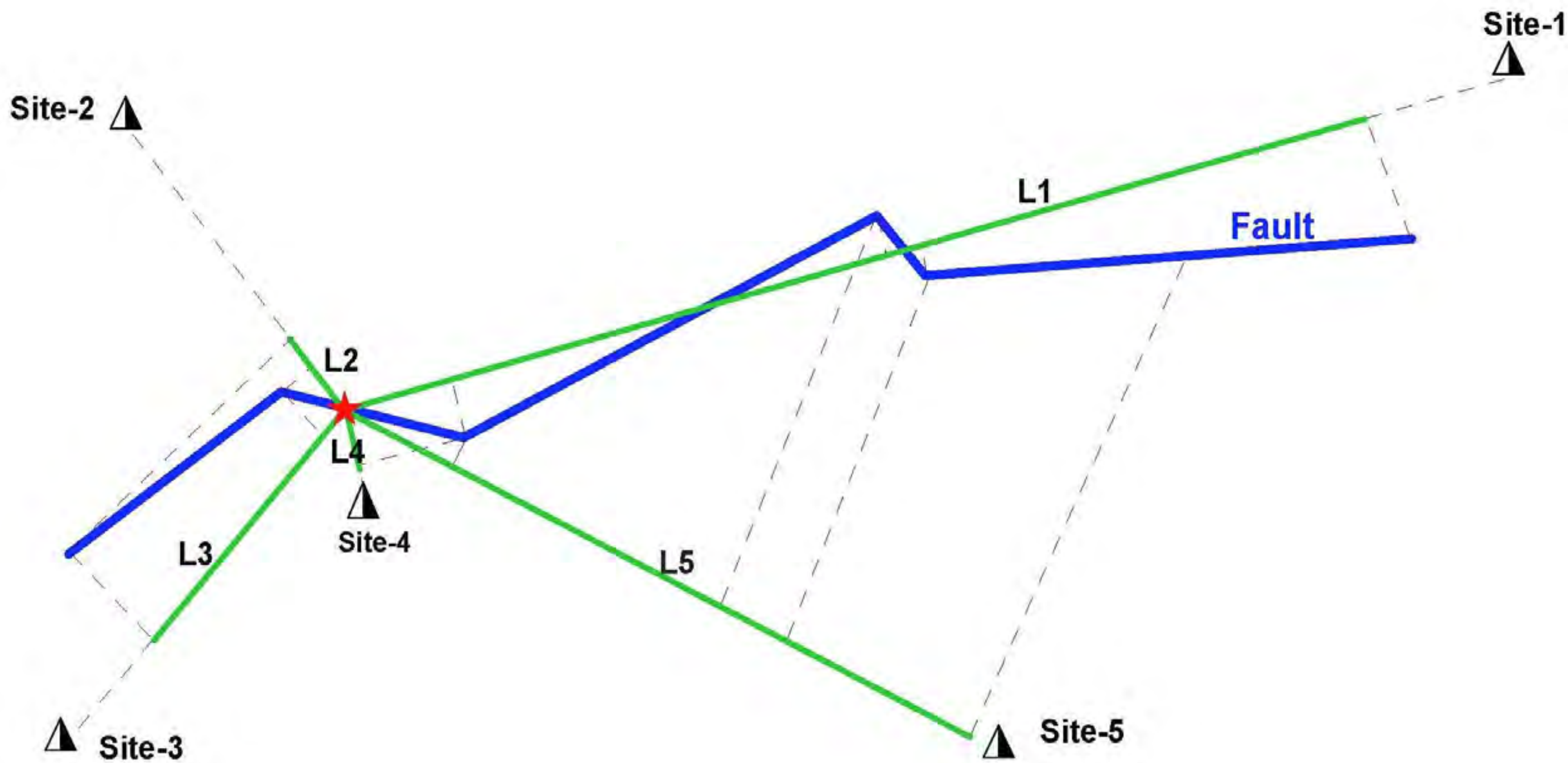

Compute "*Lr*" for a Site

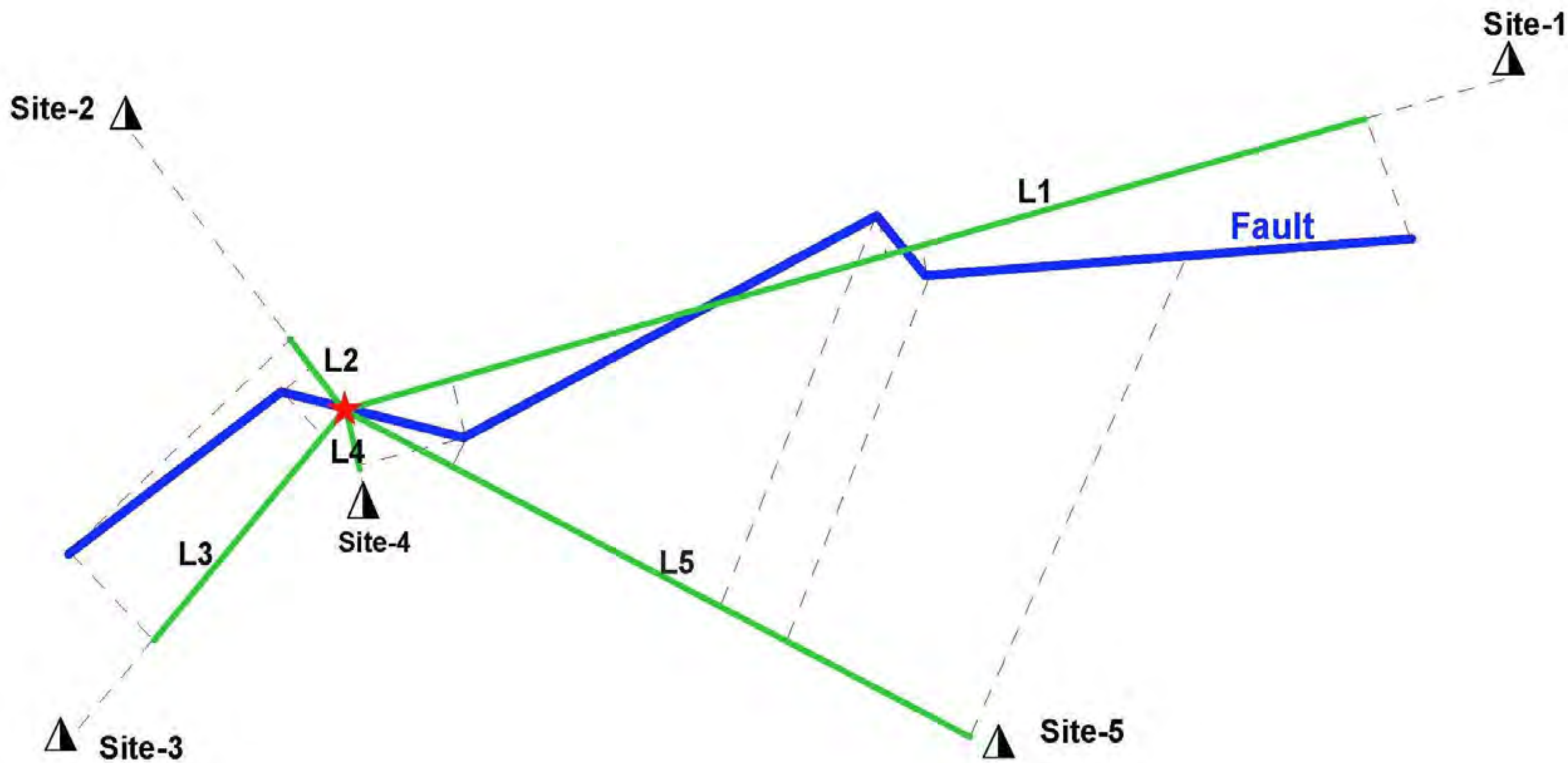

Distance Taper: A Period-Independent Taper is Applied on the Sub-Fault; A Period-Dependent Distance Taper May be Applied by the Developers to Capture Higher Correlations

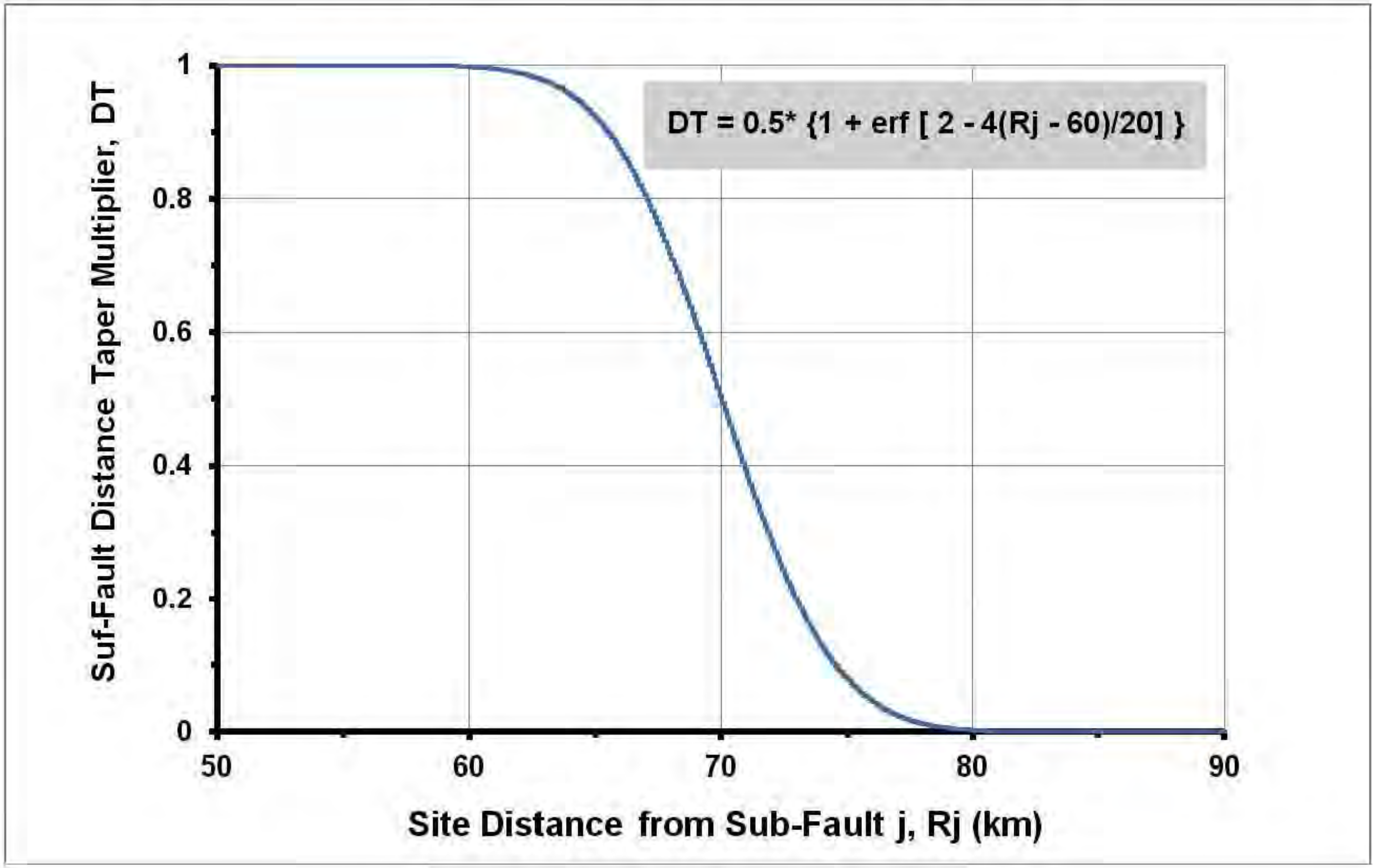

Change in intra-event sigma caused by inclusion of Rowshandel directivity model

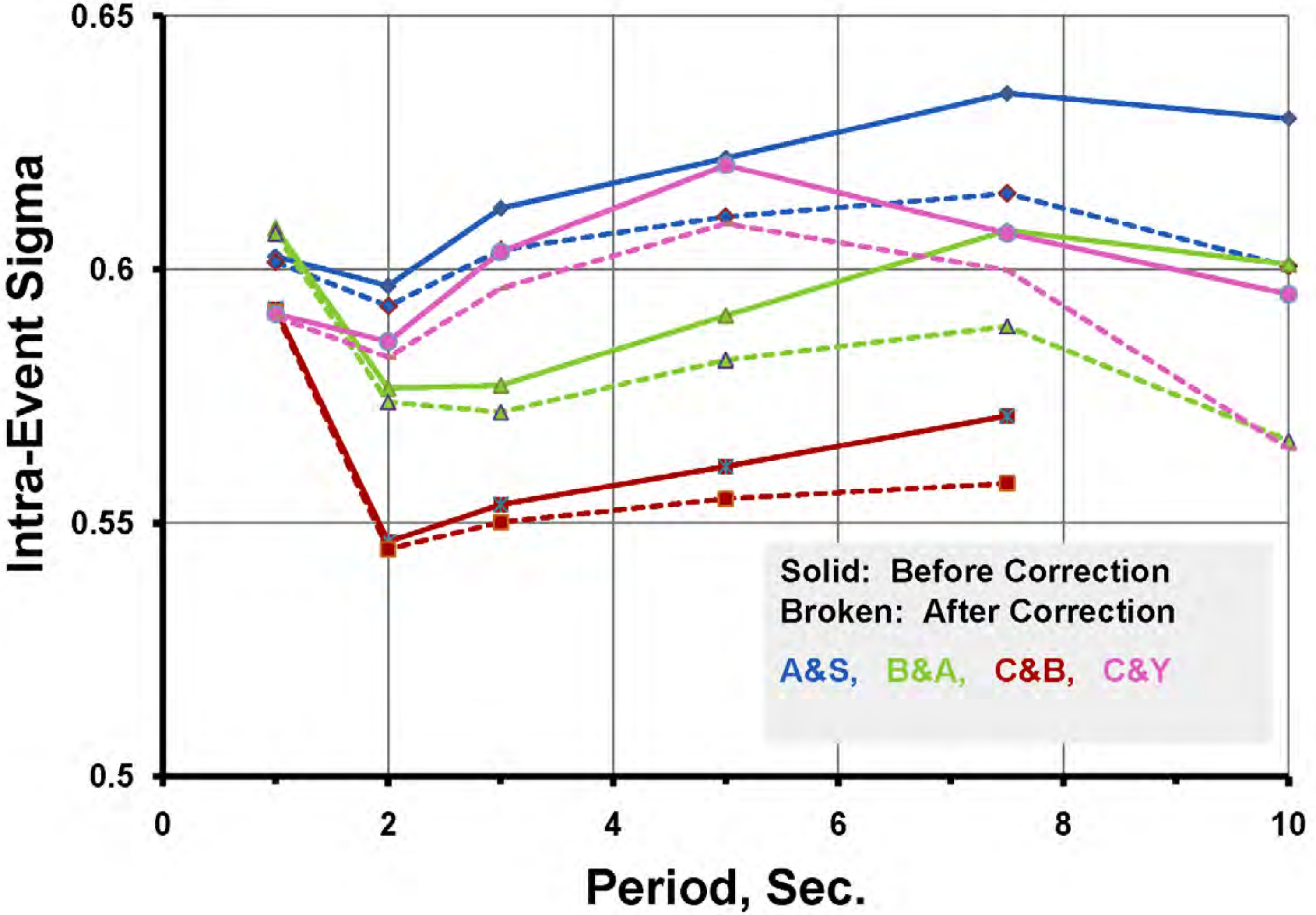

Reduction in intra-event sigma caused by inclusion of Rowshandel directivity model

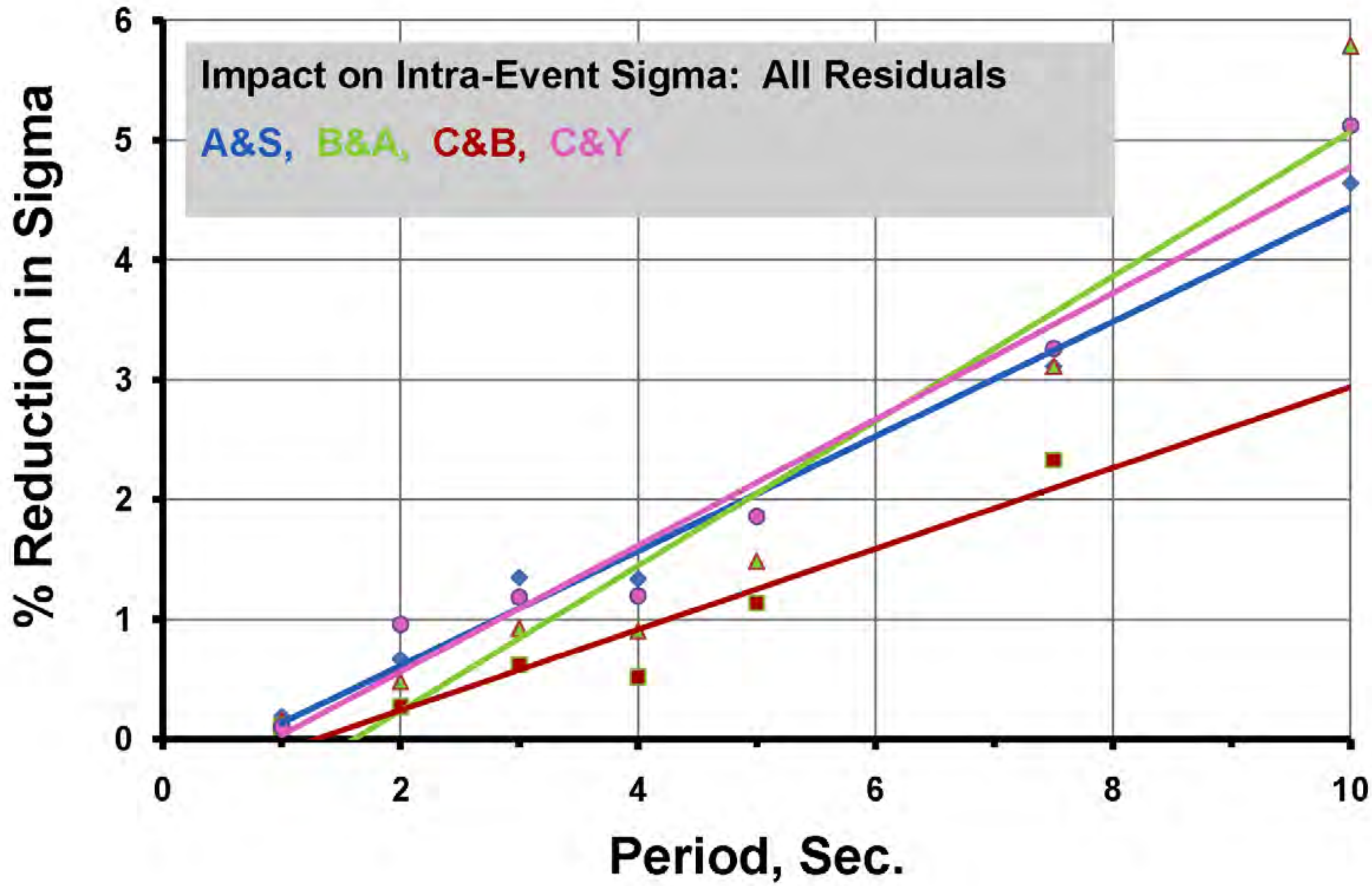

Equations

$$\ln(Sa_{dir}) = \ln(Sa) + f_D$$

$$f_D = f_D(s, \theta, d, R_x, M_w, R_{rup}, L, W, Az, T) = (C_0 + C_1 * f_{geom}) * T_{CD} * T_{M_w} * T_{Az}$$

$C_{s0}, C_{s1}, C_{d0}, C_{d1}$ = *Period dependent constant coefficient* (C_s *for strike slip*, C_d *for dip slip*)

s = *the length of striking fault rupturing towards site*; $\max[(X * L), \exp(1)]$

θ = *SSGA97 parameter* $(0° \leq \theta_1 \leq 90°)$

d = *the width of dipping fault rupturing towards site*; $\max[(Y * W), 1]$

R_x = *Horizontal distance (km) from top edge of rupture.*

W = *fault width (km)*, *note:* $\left(-\pi/2 \leq \frac{R_x}{W} \leq 2\pi/3\right)$

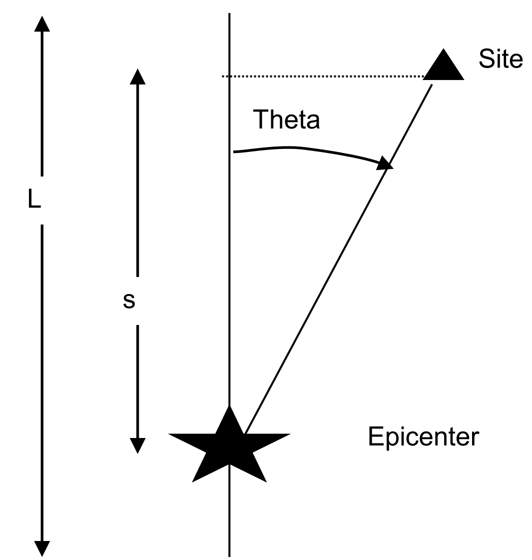

M_w = *moment magnitude*

R_{rup} = *closest distance to fault rupture plane (km)*

L = *fault length (km)*

Az = *NGA source to site azimuth*

T = *period (sec)*

Sigma

•Standard deviation of within-event residuals is recalculated after application of f_D

•Period dependent reductions are documented for each GMPE

•Reductions are calculated from only the records used in the regression. If applied to the entire flatfile (or some other set) reductions are smaller –because distance, magnitude & azimuth tapers reduce f_D to zero for many recordings

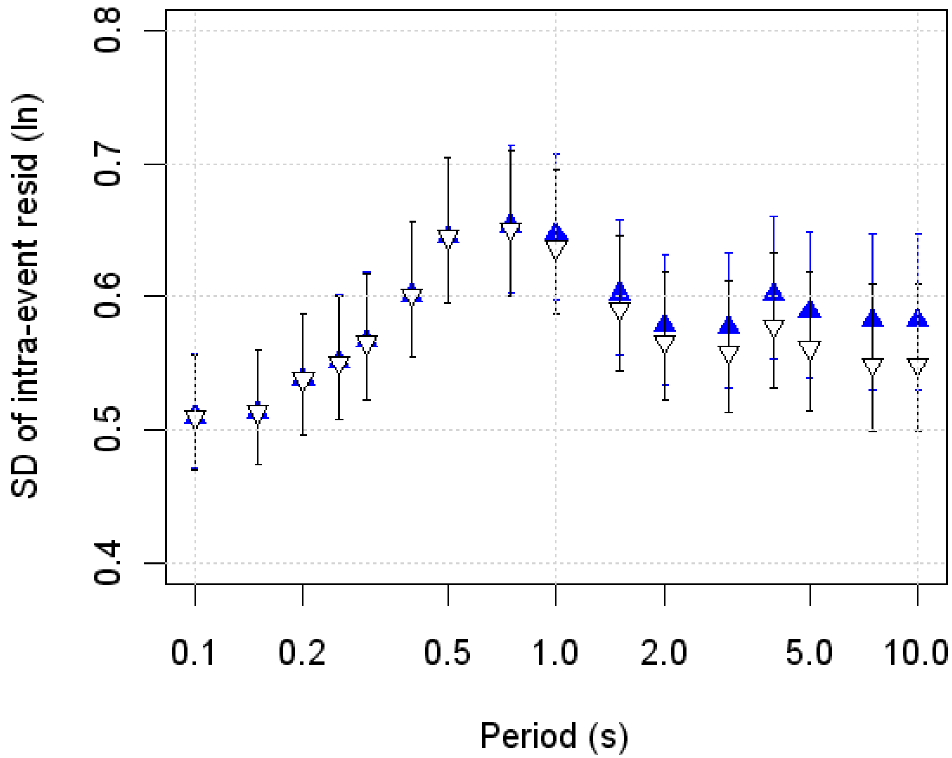

Standard deviation of within-event residuals before (solid blue triangle) and after (white triangle) directivity correction.

[CB08 GMPE, FN component, strike-slip]

Application

- Plan view of a fault and surrounding area, with heatmap colors representing predicted directivity effect, for different GM components
- Distribution of directivity effect (f_D) at T = 5.0 sec
- Hypothetical **strike slip fault** (vertical black line)
- L = 60 km, W = 15 km
- M = 7.0
- Rupture initiation point 10 km from northern end (red triangle)

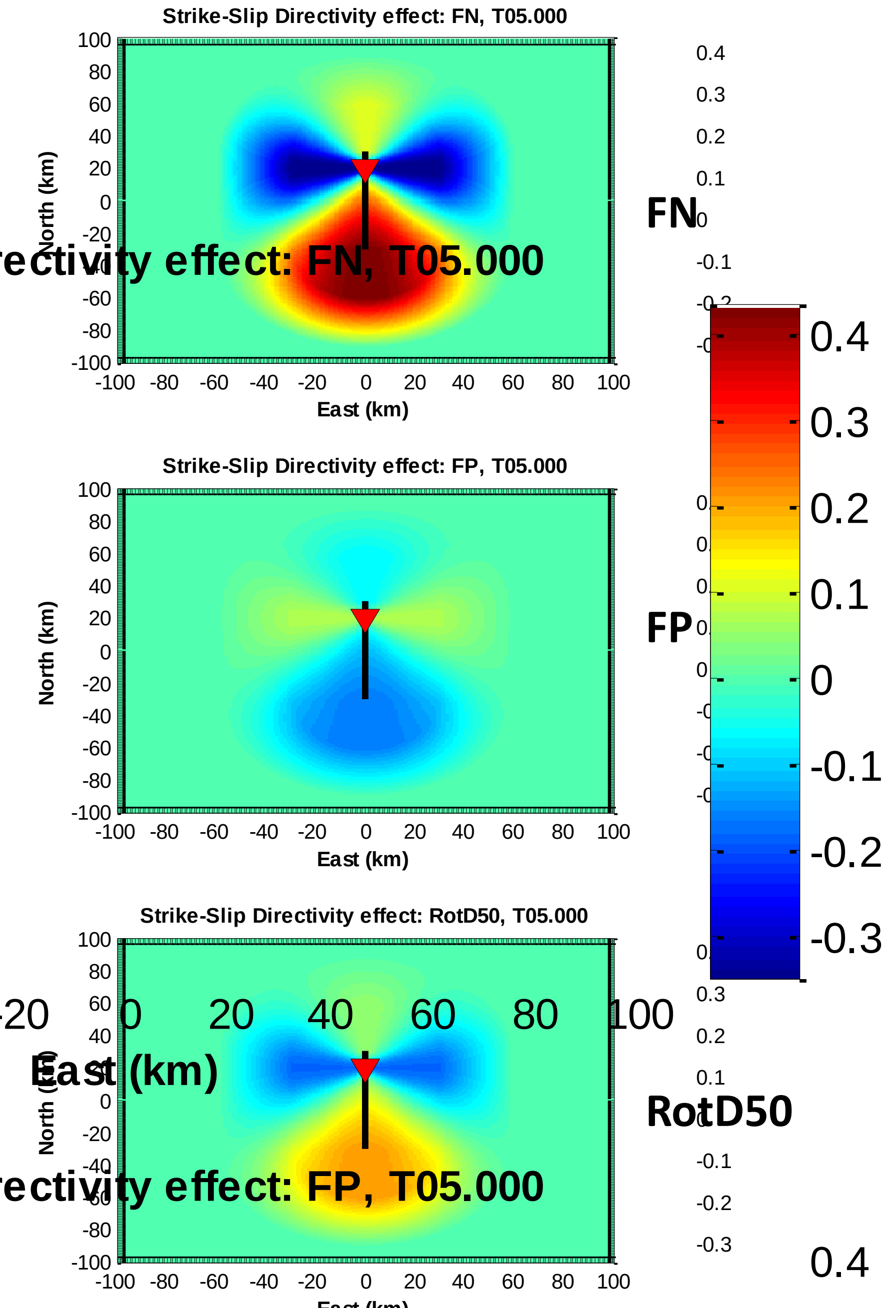

***exp(0.4)=1.49, or a maximum 49% increase on predicted GM in the FN component in this scenario**

CBSB and CBR comparison when pulse probability, period unknown

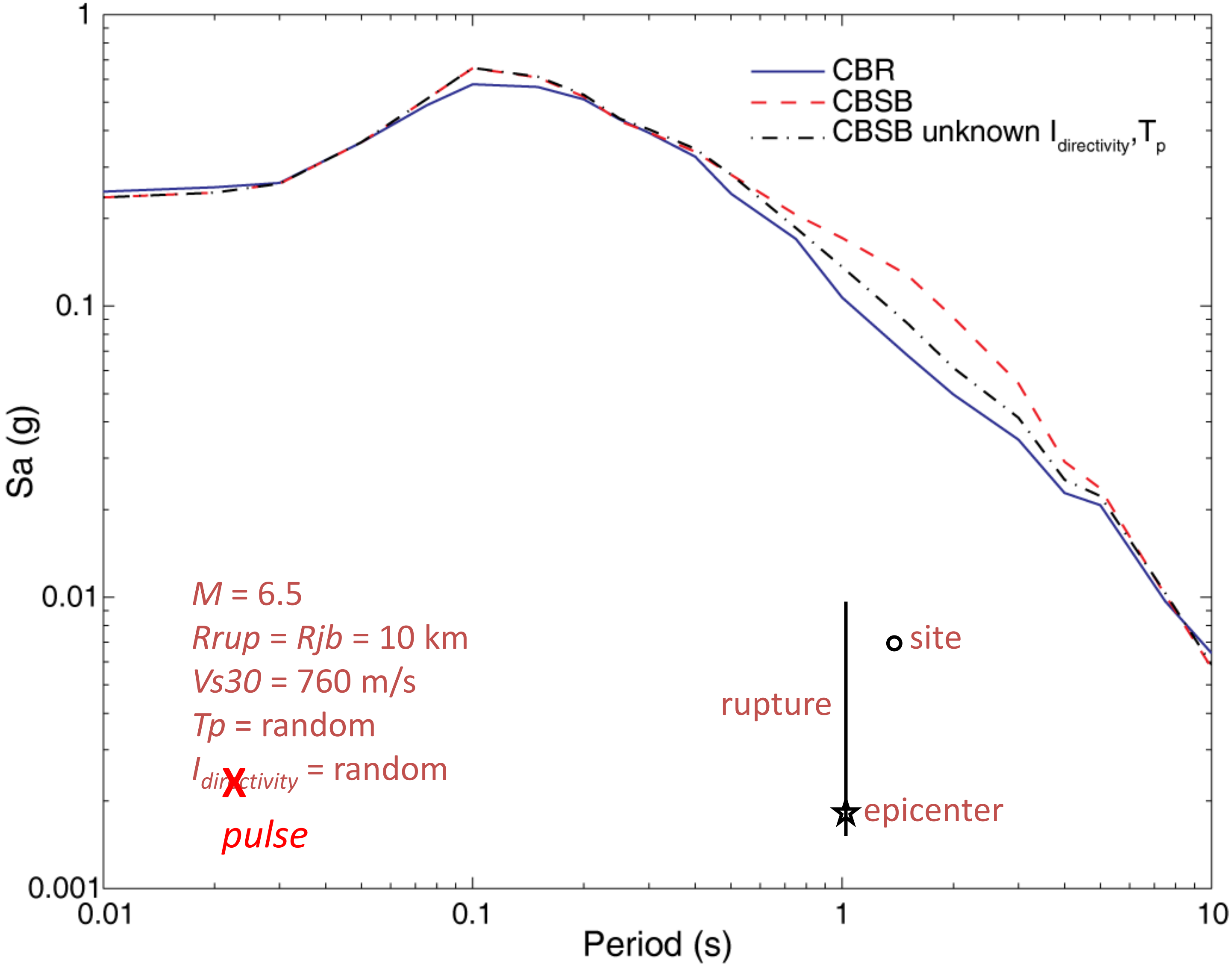

CBSB and CBR agree at two sites when there is no pulse

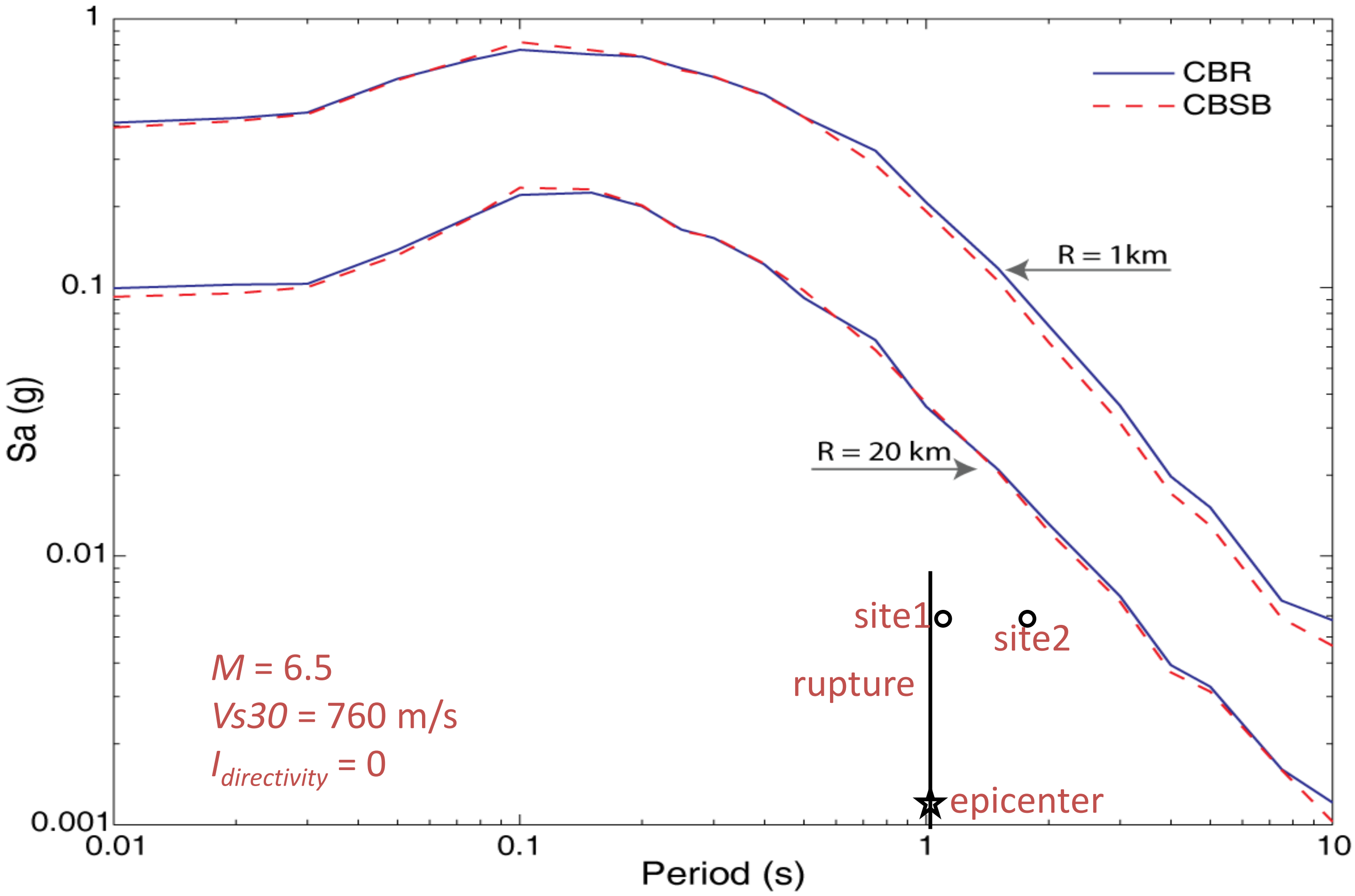

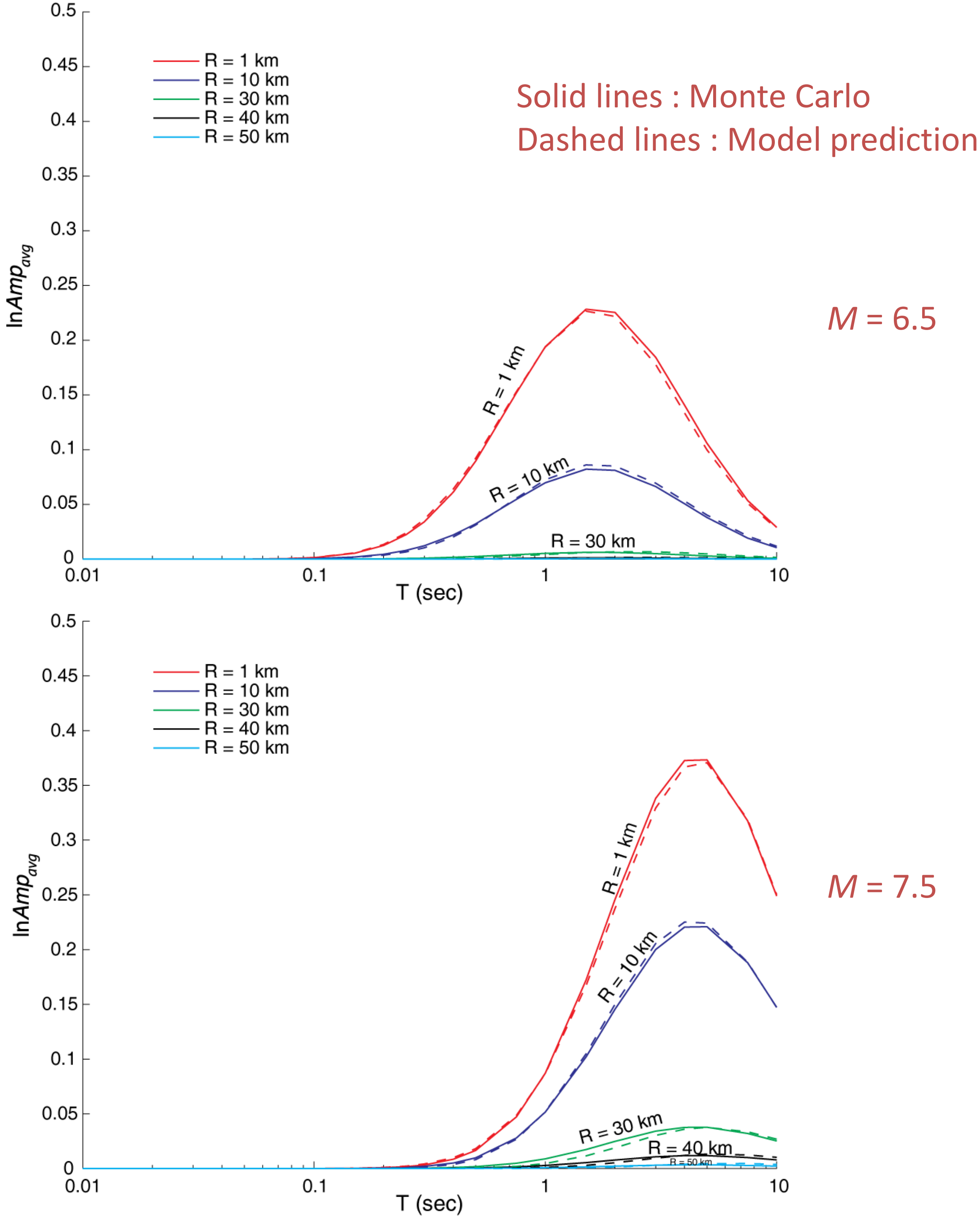

Solid lines : Monte Carlo
Dashed lines : Model prediction
M = 6.5
M = 7.5
lnAmp_avg
T (sec)
R = 1 km
R = 10 km
R = 30 km
R = 40 km
R = 50 km

CBSB using average pulse model at R= 1 km agrees with nondirective CBR prediction

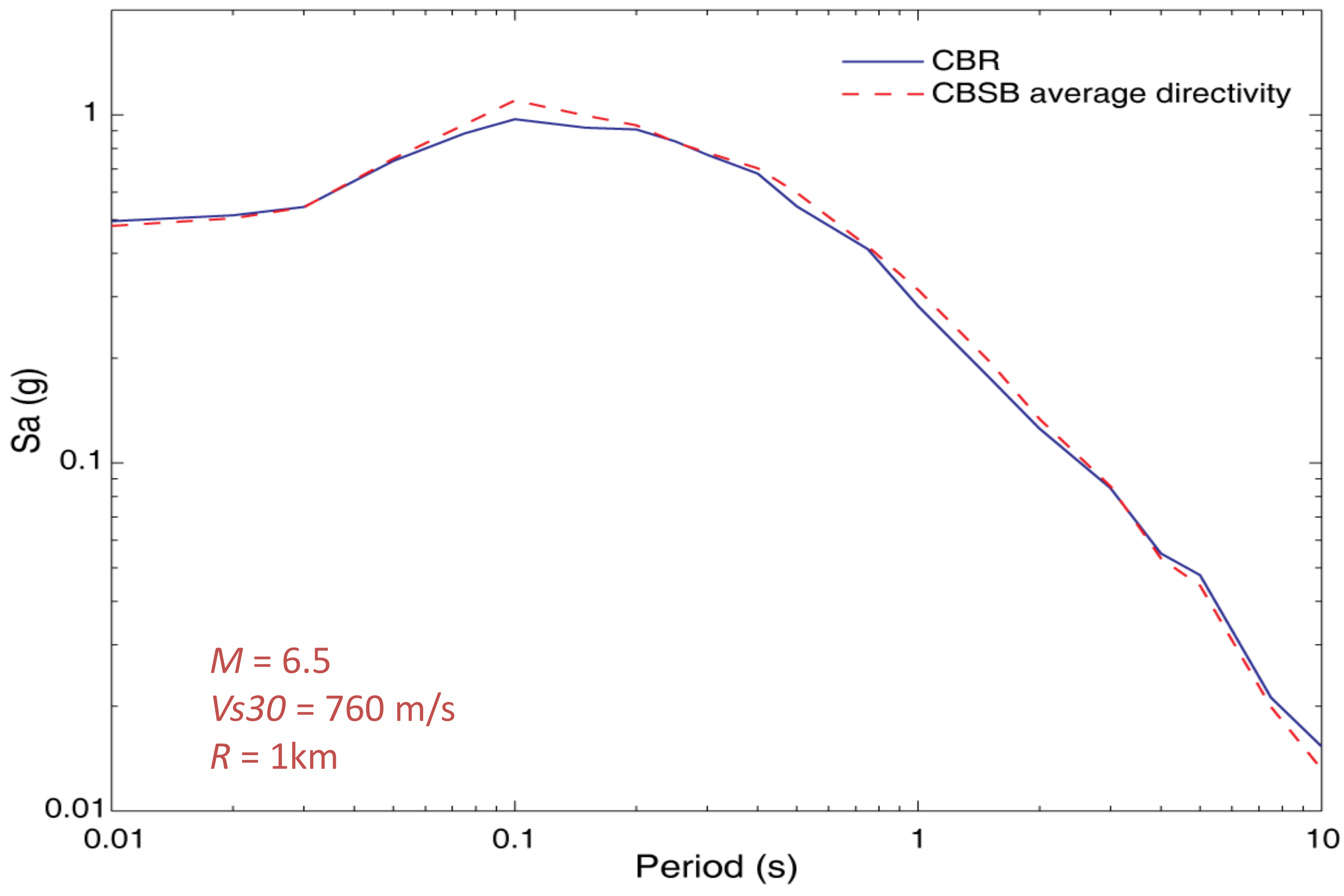

50, Imperial Valley−06, rjb <= 40, CB, intra−event resids obs g.m. / isotropic pred, 3 s
records_11mar11g.mat, resids from CB_GMRotI50_S4_03292011

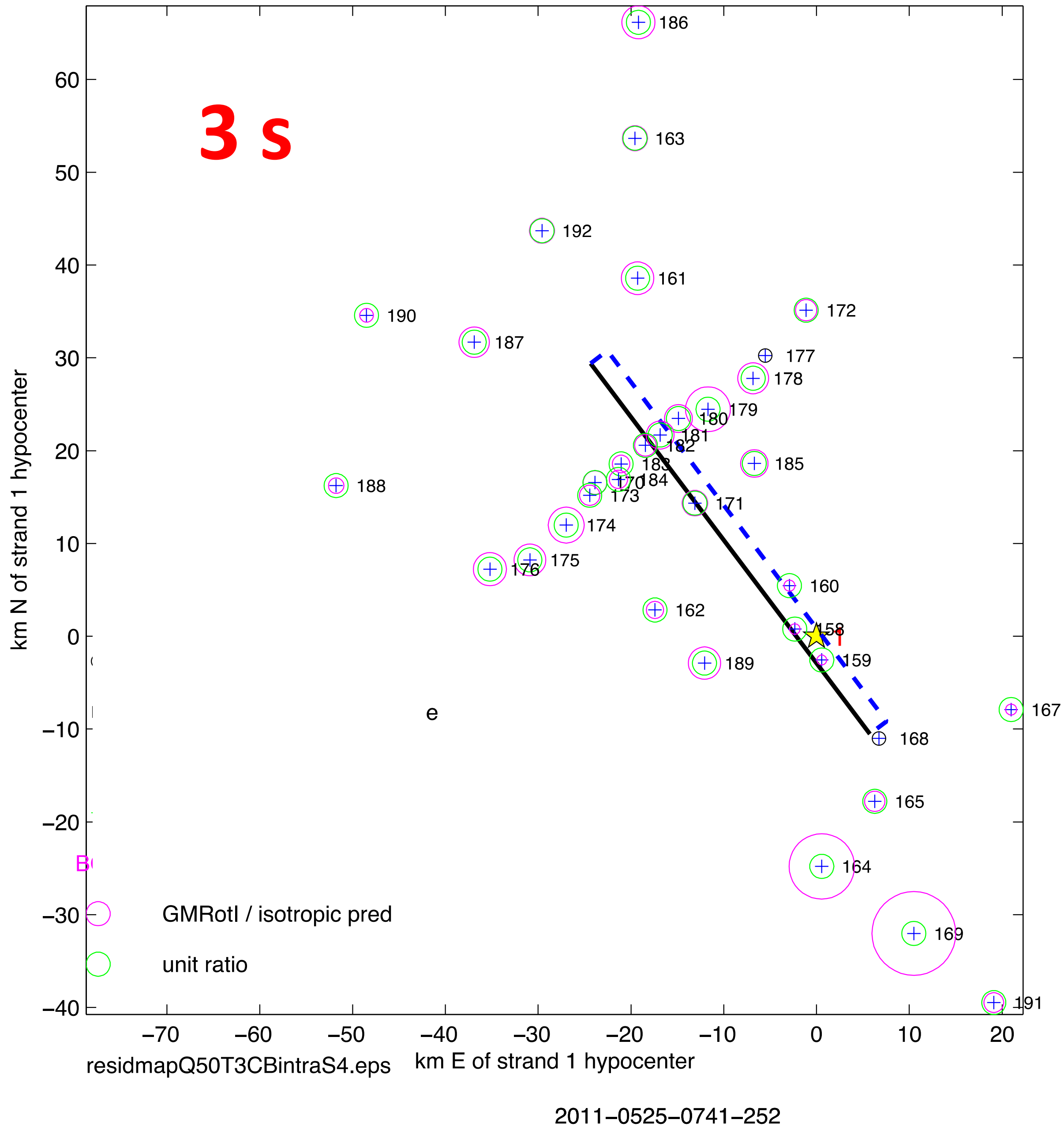

Map of intra-event residuals of gmroti50 at 3s from Campbell and Bozorgnia (2008) for the 1979 Imperial Valley earthquake

Magenta circles indicate residual –

Magenta diameter bigger/smaller than green => observed g.m. bigger/smaller than CB GMPE

CB2008 GMPE fits near fault motions well => directivity being modeled by something else in the GMPE.

Model standard deviation

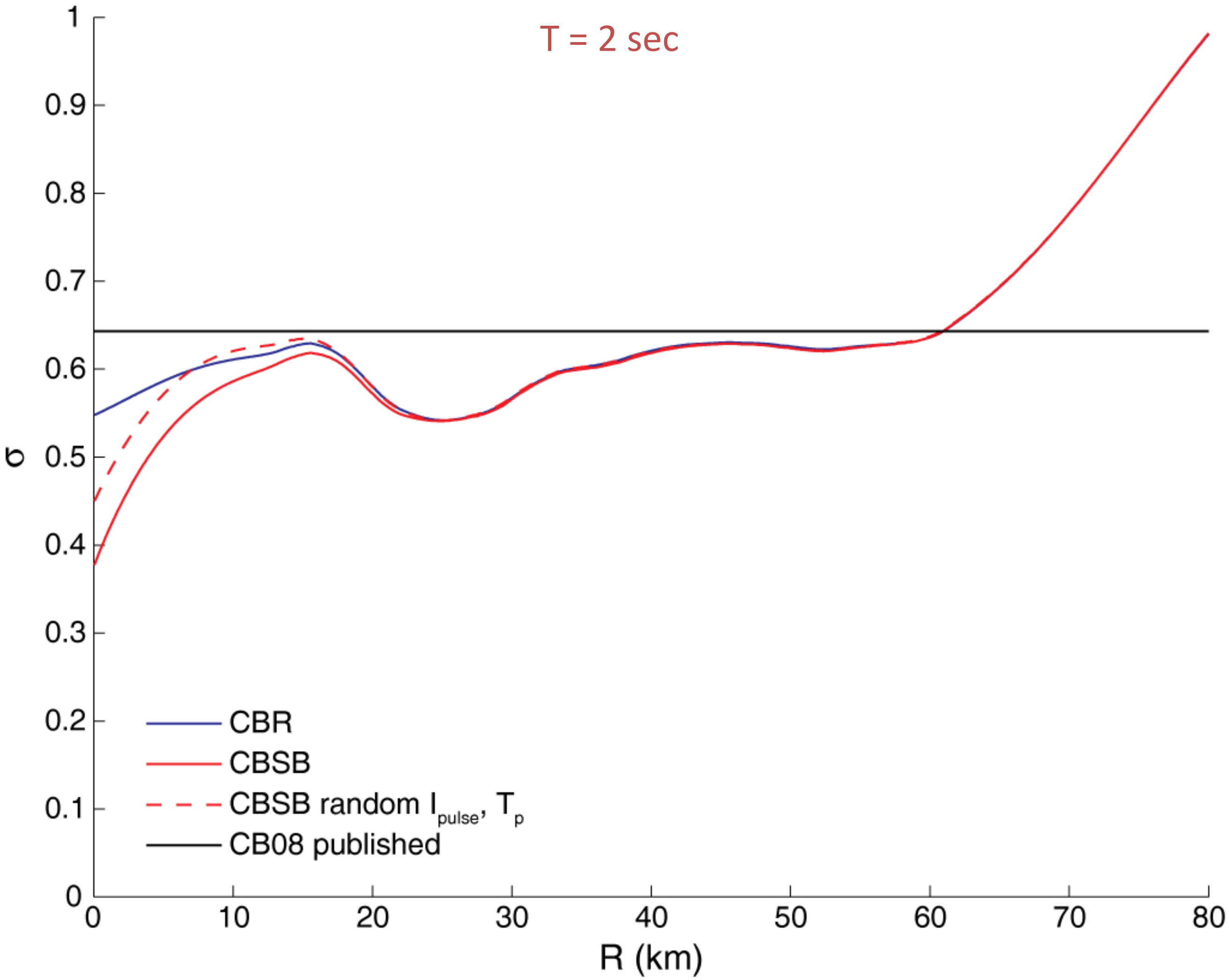

$$b/b_{max} = e^{-[\log_{10}(T/T_{max})]^2/2(0.4)^2}$$

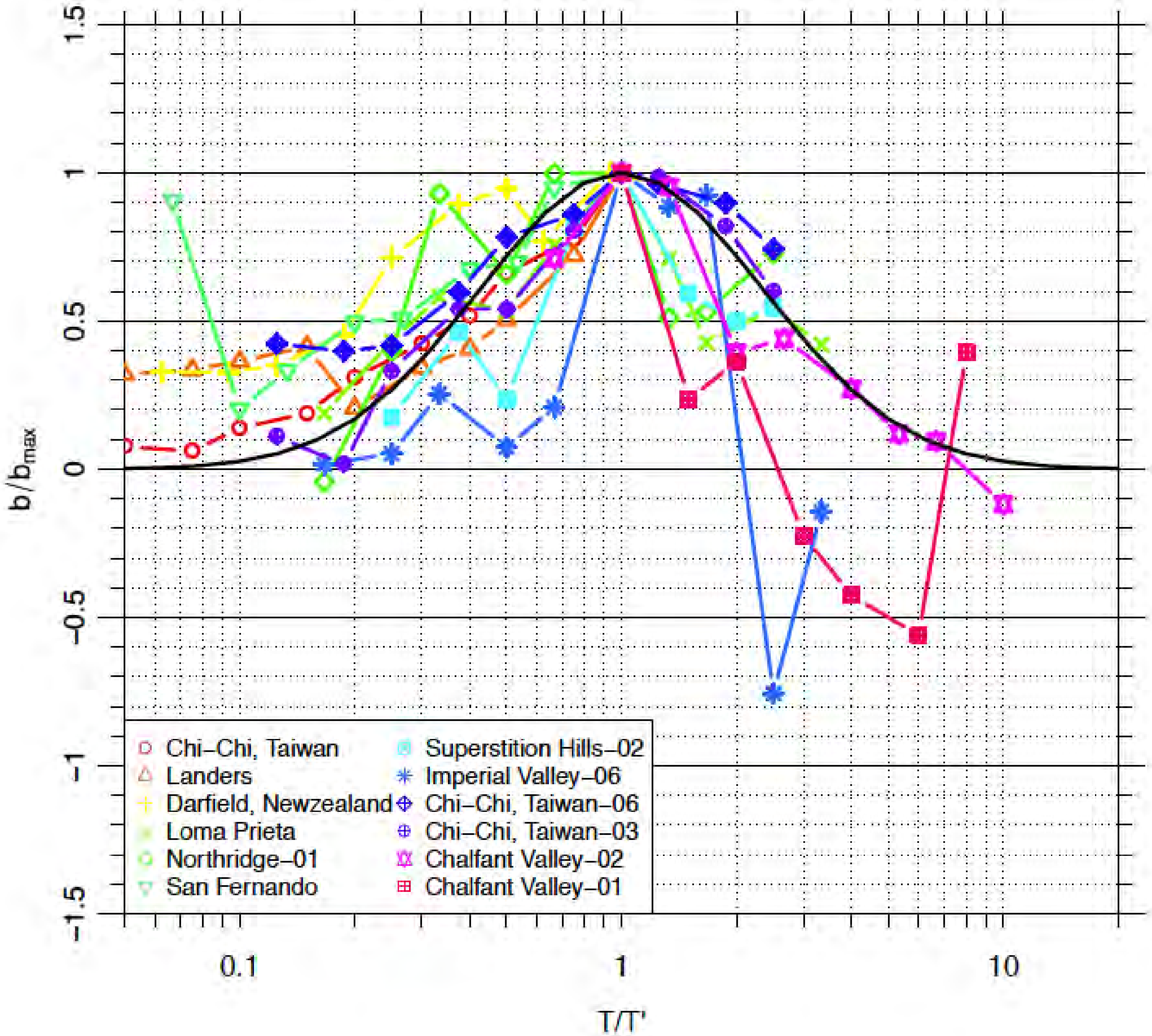

Magnitude dependence of b_{max}, max coeff.

$$b_{\max} = \quad 785 + \quad 655 \ \max(M - 6.2,\ 0)$$

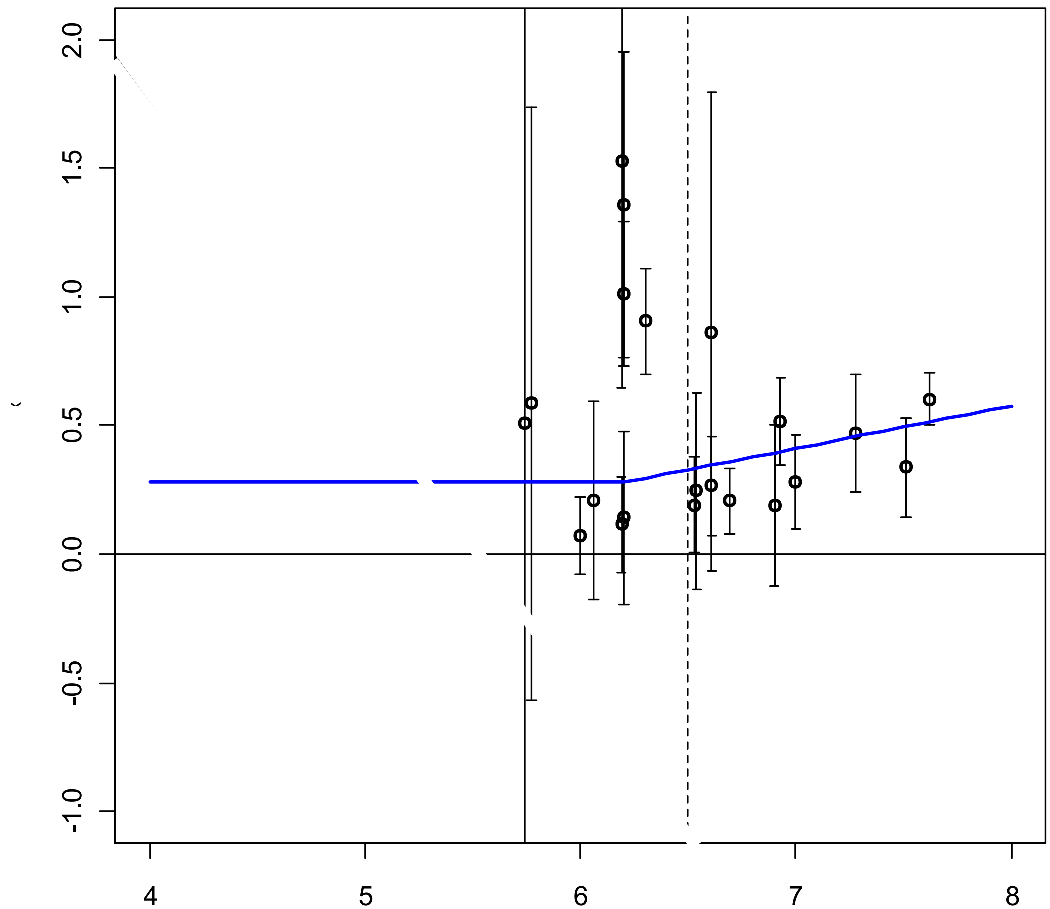

In the regression model (model 3) (later) the functional form is the same but the coefficients change

6Jan2012

Magnitude dependence of T_{max}, period of peak b

$$\log_{10}(T_{\max}) = -\text{[illegible]}884 + \text{[illegible]}479M$$

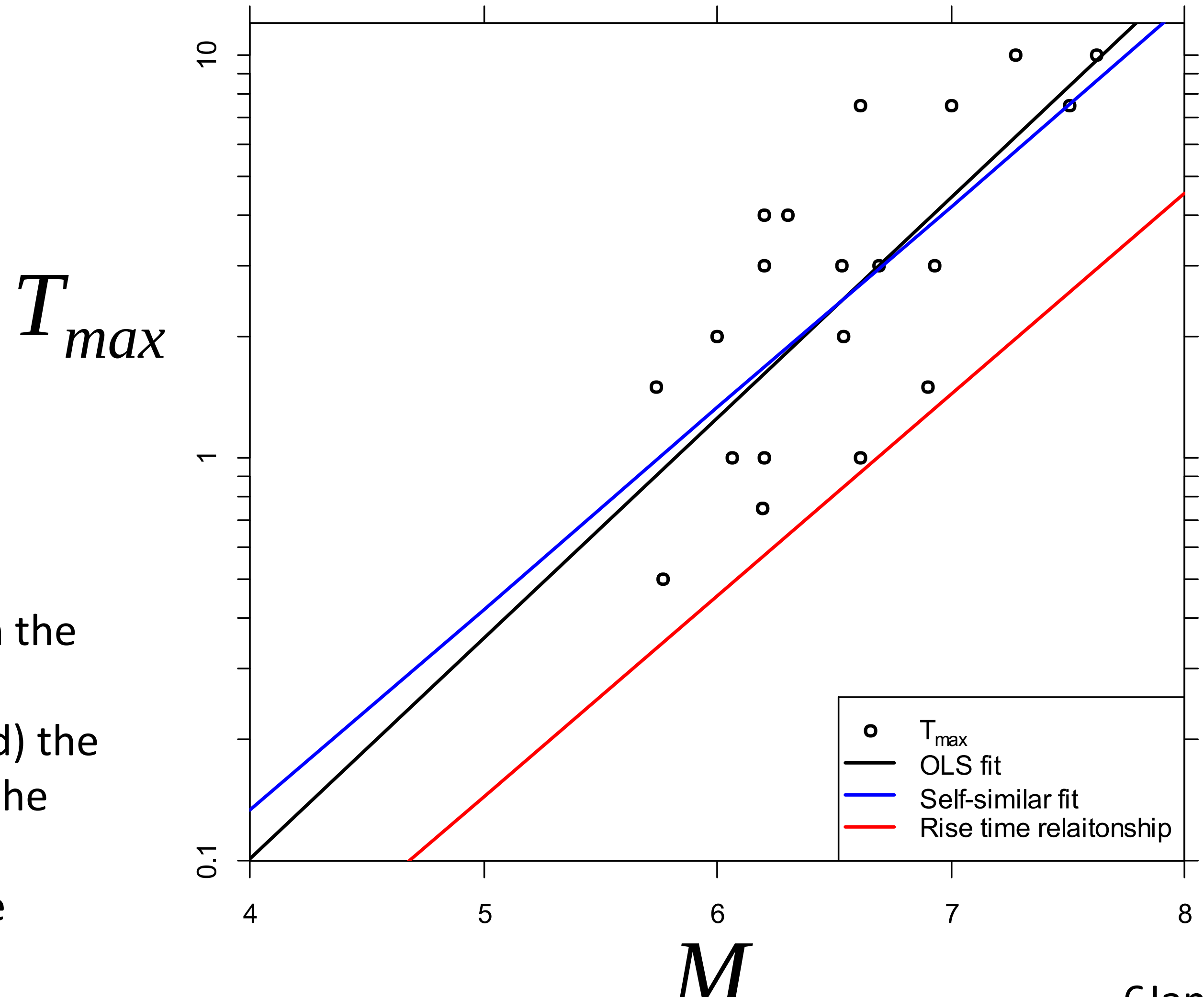

Model 1 shown. In the regression model (model 3, preferred) the functional form is the same but the coefficients change

6Jan2012

Predictive model for average IDP as a function of target fault length and mechanism

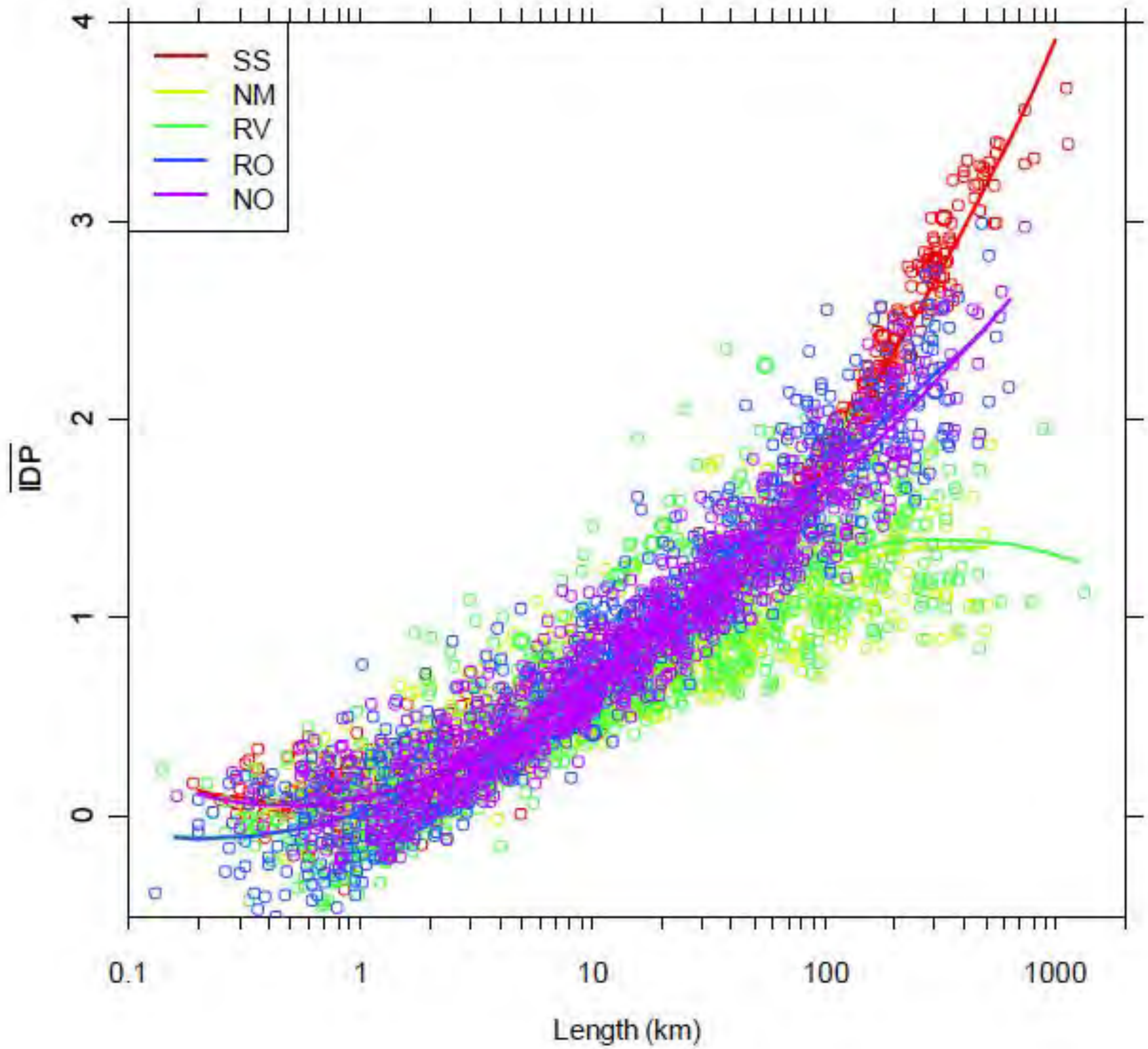

Figure 346-1. Scatter plot of the average IDP from 4,500 simulated faults against fault length. Solid lines are the fitted curves for various mechanisms.

Spudich and Chiou IEP model

(Coming soon)